

Solving for the low-rank tensor components of a scattering wave function

Jacob Snoeijer and Wim Vanroose

March 22, 2022

Abstract

Atomic and molecular breakup reactions, such as multiple-ionisation, are described by a driven Schrödinger equation. This equation is equivalent to a high-dimensional Helmholtz equation and it has solutions that are outgoing waves, emerging from the target. We show that these waves can be described by a low-rank approximation. For 2D problems this is a matrix product of two low-rank matrices, for 3D problems it is a low-rank tensor decomposition. We propose an iterative method that solves, in an alternating way, for these low-rank components of the scattered wave. We illustrate the method with examples in 2D and 3D.

1 Introduction

An in-coincidence experiment measures simultaneously the outgoing momenta of multiple products of a microscopic reaction [21]. It is an instrument that can study the correlations in reactions involving multiple particles. In double ionization, for example, a single photon ionizes, simultaneously, two electrons and the outgoing momenta of both particles are captured [1]. The reaction probes the correlation between two electrons in, for example, a chemical bond at the moment of photon impact. The outgoing wave of the two electrons is described by a 6D correlated wave and results in a cross section that depends on four angles, the directions of the first and the second electron.

Free-electron lasers, and similar experiments around the world, are expected to generate a wealth of this high-dimensional scattering data. This will result in high-dimensional forward and inverse wave problems that need to be solved to interpret the data.

The experimental cross section are often smooth functions as a function of the angles. Similarly, some parts of the scattering solution, such as single-ionization, only probes a limited subspace of the possible full solution space. The scattering solution can then be described by a low-rank wave function, a product of one-particle bound states with scattering waves in the other coordinates.

This paper introduces a low-rank representation for the scattering solutions, not only for the single ionization but also for double and triple ionization waves that appear in breakup reaction.

We also propose and analyze an alternating direction algorithm that directly solves for the low-rank components that describe the solution. This reduces a large-scale linear system to smaller, low-dimensional, scattering problems that are solved in an iterative sequence. The proposed method can be generalized to high-dimensional scattering problems where a low-rank tensor decomposition is used to represent the full scattering wave function. Efficient low-rank tensor representations are used in quantum physics for quite some time already [11, 14]. They are also used in the applied mathematics literature to approximate high-dimension problems, for a review see [8, 9, 12]. Methods such ALS [10], DMRG [16], and AMEn [6] use in alternating directions, a small linear system to determine the low-rank components of a tensor decomposition. These innovations have not found their application in computational scattering theory.

To calculate cross sections, from first principles, we start from a multi-particle Schrödinger equation. The equation is reformulated into a driven Schrödinger equation with an unknown scattering wave function and a right hand side that describes the excitation, for example, a dipole operator working on the initial state.

Since the asymptotic behaviour of a scattering function for multiple charged particles is in many cases unknown, absorbing boundary conditions [22, 2] are used. Here, an artificial layer is added to the numerical domain that dampens outgoing waves. The outgoing wave boundary conditions are then replaced with homogeneous Dirichlet boundary conditions at the end of the artificial layer. These boundary do not require any knowledge about the asymptotic behaviour, which becomes very complicated for these multiple charged particles.

The resulting equation is discretized on a grid and results in a large, sparse indefinite linear system. It is typically solved by a preconditioned Krylov subspace method [5]. However, the preconditioning techniques for

indefinite systems are not as efficient as preconditioners for symmetric and positive definite system. And solving the resulting equation is still a computationally expensive task, often requiring a distributed calculation on a supercomputer.

To compare the resulting theoretical cross sections with experimental data, a further postprocessing step is necessary. The cross section is the farfield map and this is calculated through integrals of the scattering wave function, which is the solution of the linear system, and a Greens function [13].

The main result of the paper is that we show that scattering waves that describe multiple ionization can be represented by a low-rank tensor. We first show this for a 2D wave and then generalize the results to 3D waves. The methodology can be generalized to higher dimension.

The outline of the paper is as follows. In section 2 we review the methodology that solves a forward scattering problem. It results in a driven Schrödinger equation with absorbing boundary conditions. From the solution we can extract the cross section using an integral. In section 3 we illustrate, in 2D, that a solution can be approximated by a truncated low-rank approximation. We also show that these low-rank components can be calculated directly with an iterative method. In section 4 we show that this methodology generalizes to 3D and higher dimensional problems. We use a truncated tensor decomposition and determine the components with a similar iterative method. A discussion of some numerical results and a comparison of the different presented versions of the method is given in section 5. In the final section, Sec. 6, we summarize some conclusions and discuss some possible extensions of the presented method.

2 State of the art

This section summarizes the methodology that solves a forward break-up problems with charged particles. The methodology is developed in a series of papers [20, 13] and applied to solve the impact-ionization problem [19] and double ionization of molecules [27, 26]. These methods are being extended to treat, for example, water [23]. The helium atom, He, is the simplest system with double ionization [3]. It has two electrons with coordinates $\mathbf{r}_1 \in \mathbb{R}^3$ and $\mathbf{r}_2 \in \mathbb{R}^3$ relative to the nucleus positioned at $\mathbf{0}$. The driven Schrödinger equation for $u(\mathbf{r}_1, \mathbf{r}_2) \in C^2$ then reads

$$\left(-\frac{1}{2}\Delta_{\mathbf{r}_1} - \frac{1}{2}\Delta_{\mathbf{r}_2} - \frac{1}{\|\mathbf{r}_1\|} - \frac{1}{\|\mathbf{r}_2\|} + \frac{1}{\|\mathbf{r}_1 - \mathbf{r}_2\|} - E \right) u(\mathbf{r}_1, \mathbf{r}_2) = \mu\phi_0(\mathbf{r}_1, \mathbf{r}_2) \quad \forall \mathbf{r}_1, \mathbf{r}_2 \in \mathbb{R}^3, \quad (1)$$

where the right hand side is the dipole operator μ working on the ground state ϕ_0 , the eigenstate with the lowest energy λ_0 . The operators $-\frac{1}{2}\Delta_{\mathbf{r}_1}$ and $-\frac{1}{2}\Delta_{\mathbf{r}_2}$ are the Laplacian operators for the first and second electron and model the kinetic energy. The nuclear attraction is $-1/\|\mathbf{r}_1\|$ and $-1/\|\mathbf{r}_2\|$ and the electron-electron repulsion is $1/\|\mathbf{r}_1 - \mathbf{r}_2\|$.

The total energy $E = h\nu + \lambda_0$ is the energy deposited in the system by the photon, $h\nu$, and the energy λ_0 of the ground state. If the $E > 0$, both electrons can escape simultaneously from the system. The solution $u(\mathbf{r}_1, \mathbf{r}_2)$ then represents a 6D wave emerging from the nucleus.

The equation can be interpreted as a Helmholtz equation with a space-dependent wave number, $k^2(\mathbf{r}_1, \mathbf{r}_2)$,

$$(-\Delta_{6D} - k^2(\mathbf{r}_1, \mathbf{r}_2)) u(\mathbf{r}_1, \mathbf{r}_2) = f(\mathbf{r}_1, \mathbf{r}_2) \quad \forall (\mathbf{r}_1, \mathbf{r}_2) \in \mathbb{R}^6. \quad (2)$$

In this paper we prefer to write this Helmholtz equation as

$$(-\Delta_{6D} - k_0^2(1 + \chi(\mathbf{r}_1, \mathbf{r}_2))) u(\mathbf{r}_1, \mathbf{r}_2) = f(\mathbf{r}_1, \mathbf{r}_2) \quad \forall (\mathbf{r}_1, \mathbf{r}_2) \in \mathbb{R}^6, \quad (3)$$

where k_0^2 is a constant wave number, in this case related to the total energy E , and a space-dependent function $\chi : \mathbb{R}^6 \rightarrow \mathbb{R}$, that goes to zero if $\|\mathbf{r}_1\| \rightarrow \infty$ or $\|\mathbf{r}_2\| \rightarrow \infty$ that represents all the potentials.

2.1 Expansion in spherical waves and absorbing boundary conditions

For small atomic and molecular system, where spherical symmetry is relevant, the system is typically written in spherical coordinates and expanded in spherical harmonics. With $\mathbf{r}_1(\rho_1, \theta_1, \varphi_1)$ and $\mathbf{r}_2(\rho_2, \theta_2, \varphi_2)$ we can write

$$u(\mathbf{r}_1, \mathbf{r}_2) = \sum_{l_1}^{\infty} \sum_{m_1=-l_1}^{l_1} \sum_{l_2=0}^{\infty} \sum_{m_2=-l_2}^{l_2} u_{l_1 m_1, l_2 m_2}(\rho_1, \rho_2) Y_{l_1 m_1}(\theta_1, \varphi_1) Y_{l_2 m_2}(\theta_2, \varphi_2), \quad (4)$$

where $Y_{l_1 m_1}(\theta_1, \varphi_1)$ and $Y_{l_2 m_2}(\theta_2, \varphi_2)$ are spherical Harmonics, the eigenfunctions of the angular part of a 3D Laplacian in spherical coordinates. In practice the sum in equation (4) is truncated. The expansion is then a low-rank, truncated, tensor decomposition of a 6D tensor describing the solution.

For each l_1, m_1, l_2 and m_2 combination, the radial function $u_{l_1 m_1, l_2 m_2}(\rho_1, \rho_2)$ describes an outgoing wave that depends on the distances ρ_1 and ρ_2 of the two electrons to the nucleus.

A coupled equation that simultaneously solves for all the $u_{l_1 m_1, l_2 m_2}(\rho_1, \rho_2)$'s is found by inserting the truncated sum in (1), multiplying with $Y_{l_1 m_1}^*(\theta_1, \varphi_1)$ and $Y_{l_2 m_2}^*(\theta_2, \varphi_2)$ and integrating over all the angular coordinates,

$$\begin{aligned} & \left(-\frac{1}{2} \frac{d^2}{d\rho_1^2} + \frac{l_1(l_1+1)}{2\rho_1^2} - \frac{1}{2} \frac{d^2}{d\rho_2^2} + \frac{l_2(l_2+1)}{2\rho_2^2} + V_{l_1 m_1, l_2 m_2}(\rho_1, \rho_2) - E \right) u_{l_1 m_1, l_2 m_2}(\rho_1, \rho_2) \\ & + \sum_{l'_1 m'_1, l'_2 m'_2} V_{l_1 m_1, l_2 m_2, l'_1 m'_1, l'_2 m'_2}(\rho_1, \rho_2) u_{l'_1 m'_1, l'_2 m'_2}(\rho_1, \rho_2) = f_{l_1 m_1, l_2 m_2}(\rho_1, \rho_2) \quad \forall l_1 m_1, l_2 m_2. \quad \forall \rho_1, \rho_2 \in [0, \infty[\end{aligned} \quad (5)$$

with boundary conditions $u(\rho_1 = 0, \rho_2) = 0$ for all $\rho_2 \geq 0$ and $u(\rho_1, \rho_2 = 0) = 0$ for all $\rho_1 \geq 0$.

The equation (5) is typically discretized on a spectral elements quadrature grid [20].

To reflect the physics, where electrons are emitted from the system, outgoing wave boundary conditions need to be applied at the outer boundaries. There are many ways to implement outgoing wave boundary conditions. Exterior complex scaling (ECS) [22] for example, is frequently used in the computational atomic and molecular physics literature. In the computational electromagnetic scattering a perfectly matched layers (PML) [2] is used, which can also be interpreted as a complex scaled grid. [4]

2.2 Calculation of the amplitudes

To correctly predict the probabilities of the arriving particles at the detector, we need the amplitudes of the solution far away from the molecule. These are related to the asymptotic amplitudes of the wave functions.

Let us go back to the formulation with Helmholtz equation, as given in (2). Suppose that we have solved the following Helmholtz equation with absorbing boundary conditions, in any representation,

$$(-\Delta - k_0^2(1 + \chi(\mathbf{x}))) u_{sc}(\mathbf{x}) = f(\mathbf{x}), \quad \forall \mathbf{x} \in [-L, L]^d, \quad (6)$$

where f is only non-zero on the real part of the grid $[-L, L]^d \subset \mathbb{R}^d$. Similarly, $\chi(\mathbf{x})$ is only non-zero on the box $[-L, L]^d$.

The calculation of the asymptotic amplitudes requires the solution $u_{sc}(\mathbf{x})$ for an \mathbf{x} outside of the box $[-L, L]^d$. To that end, we reorganize equation (6), after we have solved it, as follows

$$(-\Delta - k_0^2) u_{sc} = f + k_0^2 \chi u_{sc}. \quad (7)$$

The right hand side of (7) is now only non-zero on $[-L, L]^d$, since both f and χ are only non-zero there. Furthermore, since we have solved (6) we also know u_{sc} on $[-L, L]^d$. So the full right hand side of (7) is known. The remaining left hand side of (7) is now a Helmholtz equation with a constant wave number k_0^2 . For this equation the Greens function is known analytically.

$$\begin{aligned} u_{sc}(\mathbf{x}) &= \int G(\mathbf{x}, \mathbf{y}) (f(\mathbf{y}) + k_0^2 \chi(\mathbf{y}) u_{sc}(\mathbf{y})) d\mathbf{y} \\ &= \int_{[-L, L]^d} G(\mathbf{x}, \mathbf{y}) (f(\mathbf{y}) + k_0^2 \chi(\mathbf{y}) u_{sc}(\mathbf{y})) d\mathbf{y} \quad \forall \mathbf{x} \in \mathbb{R}^d, \end{aligned} \quad (8)$$

where f and χ are limited to $[-L, L]^d$ thus we can truncate the integral to the box $[-L, L]^d$.

This methodology was successfully applied to calculate challenging break up problems, for example [19].

2.3 Single ionization versus double ionization

Let us discuss the qualitative behaviour of the solution for single and double ionization. To illustrate the behaviour, we truncate the partial wave expansion, (4), to the first term. This is known as a s -wave expansion. The 6D wave function is then approximated as

$$u(\mathbf{r}_1, \mathbf{r}_2) \approx u(\rho_1, \rho_2) Y_{00}(\theta_1, \varphi_1) Y_{00}(\theta_2, \varphi_2). \quad (9)$$

The radial wave, $u(\rho_1, \rho_2)$, then fits a 2D Helmholtz equation

$$\left(-\frac{1}{2} \frac{d^2}{d\rho_1^2} - \frac{1}{2} \frac{d^2}{d\rho_2^2} + V_1(\rho_1) + V_2(\rho_2) + V_{12}(\rho_1, \rho_2) - E \right) u(\rho_1, \rho_2) = f(\rho_1, \rho_2), \quad \forall \rho_1, \rho_2 \in [0, \infty[, \quad (10)$$

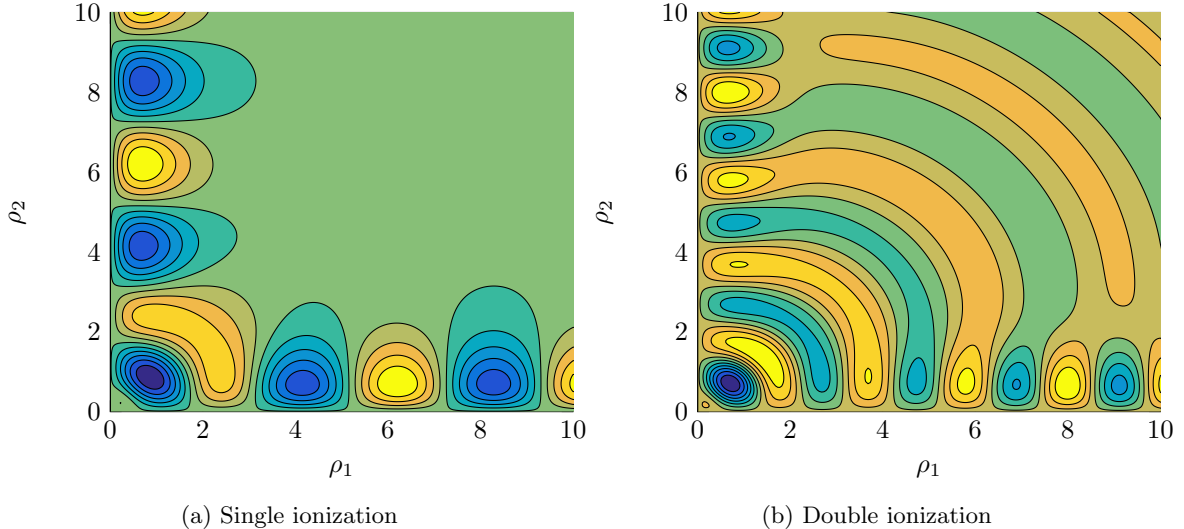


Figure 1: Left: When the energy $E = \hbar\nu + \lambda_0 < 0$, there is only single ionization. The solution is then localized along the edges, where the solution is a combination of an outgoing wave in the ρ_1 and a bound state in ρ_2 , or vice-versa. Right: For energy $E > 0$, there is, in addition to single ionization with solution localized along the edges, a double ionization wave where both coordinates can become large.

where $V_1(\rho_1)$ and $V_2(\rho_2)$ represents the one-particle potentials and $V_{12}(\rho_1, \rho_2)$ the two-particle repulsion. This model is known as a s -wave or Temkin-Poet model [24, 18].

Before the photo-ionization, the atom is in a two-particle ground state. In this s -wave model, it is the eigenstate of

$$\left(-\frac{1}{2} \frac{d^2}{d\rho_1^2} - \frac{1}{2} \frac{d^2}{d\rho_2^2} + V_1(\rho_1) + V_2(\rho_2) + V_{12}(\rho_1, \rho_2) \right) \phi_0(\rho_1, \rho_2) = \lambda_0 \phi_0(\rho_1, \rho_2). \quad (11)$$

with the lowest energy. Simultaneously, there are one-particle states that are eigenstates of

$$\left(-\frac{1}{2} \frac{d^2}{d\rho_1^2} + V_1(\rho_1) \right) \phi_i(\rho_1) = \mu_i \phi_i(\rho_1) \quad (12)$$

and

$$\left(-\frac{1}{2} \frac{d^2}{d\rho_2^2} + V_2(\rho_2) \right) \varphi_i(\rho_2) = \nu_i \varphi_i(\rho_2). \quad (13)$$

When (10) is solved with the energy $E = \hbar\nu + \lambda < 0$, there is only single ionization. Only one of the two coordinates ρ_1 or ρ_2 can become large and the solution, as can be seen in Figure 1a, is localized along both axis. The solution is a product of an outgoing wave in one coordinate and a bound state in the other coordinate. For example, along the ρ_2 -axis, the solution is described by $A_i(\rho_2)\phi_i(\rho_1)$, where $A_i(\rho_2)$ is a one-dimensional outgoing wave, with an energy $E - \mu_i$ and $\phi_i(\rho_1)$ is a bound state of (12) in the first coordinate with energy μ_i . Similarly, there is a wave, along the ρ_1 axis, that is an outgoing wave of the form $B_l(\rho_1)\varphi_l(\rho_2)$, with a scattering wave in the first coordinate, ρ_1 , and a bound state in the coordinate ρ_2 , solution of (13).

When (10) is solved with energy $E = \hbar\nu + \lambda \geq 0$ there is also double ionization and both coordinates ρ_1 and ρ_2 can become large. We see, in Figure 1b, a (spherical) wave in the middle of the domain, where both coordinates can be become large. To describe this solution the full coordinate space is necessary. Note that these solutions still show single ionization along the axes. Even for $E > 0$, one particle can take away all the energy and leave the other particle as a bound state.

2.4 Coupled channel model for single ionization waves

In this section, we write the single ionization solution as a low-rank decomposition and derive the equations for the low-rank components. When there is only single ionization, the total wave can be written as

$$u(\rho_1, \rho_2) = \sum_{m=1}^M \phi_m(\rho_1) A_m(\rho_2) + \sum_{l=1}^L B_l(\rho_1) \varphi_l(\rho_2), \quad (14)$$

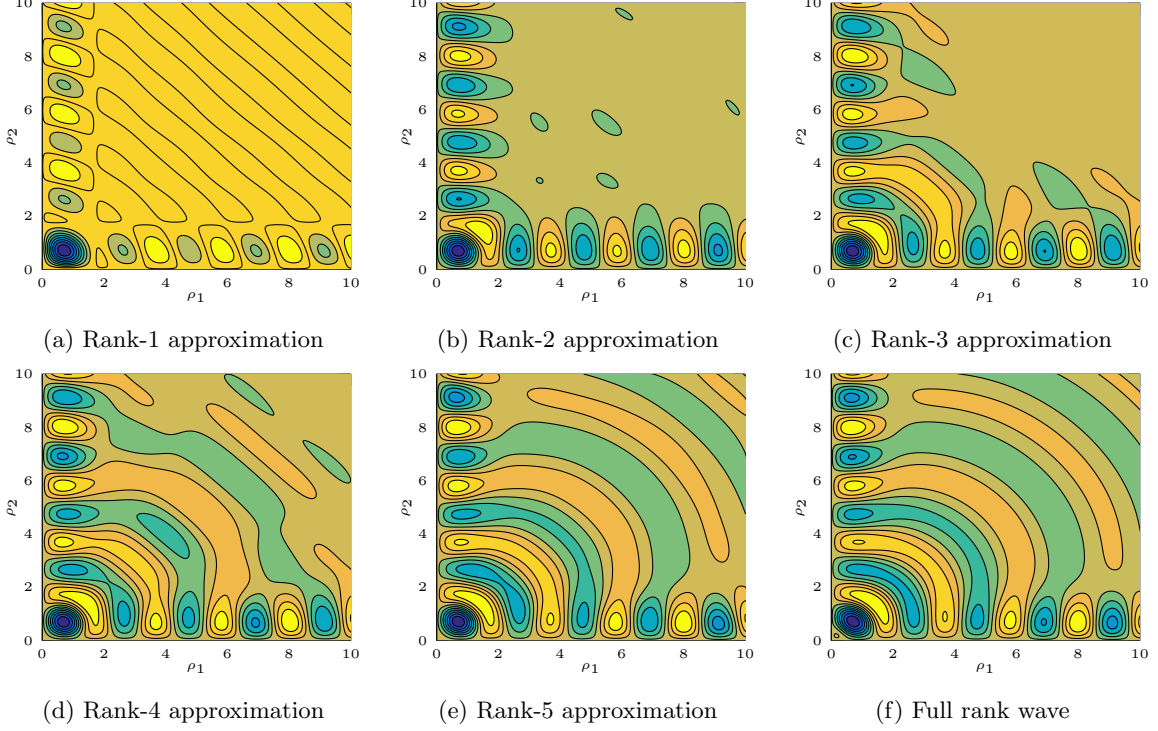


Figure 2: Contour plots of the double ionization wave function (bottom, right) and low-rank approximations for increasing rank.

where $\phi_m(\rho_1)$ and $\varphi_l(\rho_2)$ are the bound state eigenstates, defined in (12) and (13). The first term is localized along the ρ_2 -axis, the second term is localized along the ρ_1 -axis with $\mu_i < 0$ and $\nu_i < 0$.

As discussed in [5], this expansion is not unique. We can add multiples of $\gamma_i \varphi_i(\rho_2)$ to $A_i(\rho_2)$ and simultaneously subtract $\gamma_l \phi_l(\rho_1)$ from $B_l(\rho_1)$ without contaminating the result. Indeed, for any choice of $\gamma_i \in \mathbb{C}$ and $L = M$ holds that

$$u(\rho_1, \rho_2) = \sum_{m=1}^M \phi_m(\rho_1) (A_m(\rho_2) + \gamma_m \varphi_m(\rho_2)) + \sum_{l=1}^L (B_l(\rho_1) - \gamma_l \phi_l(\rho_1)) \varphi_l(\rho_2) = u(\rho_1, \rho_2). \quad (15)$$

To make the expansion unique, [5] chooses to select $A_i \perp \varphi_j$ when $j \geq i$ and $B_i \perp \phi_m$ when $i \geq j$.

In this paper, we choose to make the functions in the set $\{\phi_i \in \{1, \dots, m\}, B_l \in \{1, \dots, L\}\}$ orthogonal. We also assume that $V_{12}(\rho_1, \rho_2) \approx \sum_{i=1}^L \sum_{l=1}^M \phi_i(\rho_1) \varphi_l(\rho_2) \int \phi_i^*(\rho_1) \varphi_l^*(\rho_2) V_{12}(\rho_1, \rho_2) d\rho_1 d\rho_2$.

Given a function $f(\rho_1, \rho_2)$, a right hand side, we can now derive the equations for A_m and B_l . When we insert the low-rank decomposition of the expansion (14), in the 2D Hamiltonian (10), multiply with ϕ_i and integrate over ρ_1 we find

$$(H_2 + \mu_j - E)A_j(\rho_2) + \sum_{l=1}^M V_{lj}(\rho_2)A_l(\rho_2) = \int_0^\infty \phi_j^*(\rho_1) f(\rho_1, \rho_2) d\rho_1, \quad \text{for } j = 1, \dots, M \quad \text{and } \forall \rho_2 \in [0, L], \quad (16)$$

with

$$V_{ij}(\rho_2) = \int_0^\infty \phi_j^*(\rho_1) V_{12}(\rho_1, \rho_2) \phi_i(\rho_1) d\rho_1. \quad (17)$$

We have used that $\phi_i \perp B_l$ to eliminate the second term in the expansion (14).

Similarly, for B_l , we find

$$(H_1 + \nu_l - E)B_l(\rho_1) + \sum_{m=1}^L W_{lm}(\rho_1)B_m(\rho_1) = \int_0^\infty \varphi_l(\rho_2) \left(f(\rho_1, \rho_2) - \sum_i^M \phi_i \phi_i^* f(\rho_1, \rho_2) \right) d\rho_2 \quad (18)$$

for $i = 1, \dots, M, \quad \forall \rho_1 \in [0, \infty[$

where

$$W_{lk}(\rho_1) := \left(\int_0^\infty \varphi_l^*(\rho_2) V_{12}(\rho_1, \rho_2) \varphi_k(\rho_2) d\rho_2 \right). \quad (19)$$

3 Low-rank matrix representation of a 2D wave function that includes both single and double ionization

3.1 Low rank of the double ionization solution

We now discuss the main result of the paper. We will derive a coupled channel equation that gives a low-rank approximation for the double ionization wave function, as shown in Figure 1b.

In section 2.4 we have shown that the single ionization wave can be represented by a low-rank decomposition. In this section, we show that also the double ionization wave can be written as a similar low-rank decomposition. We first illustrate that the solution of a 2D driven Schrödinger equation that contains both single and double ionization, it is a solution of (10) with $E > 0$, can be represented by a similar low-rank decomposition.

In Figure 3 we solve the Helmholtz equation with a space-dependent wave number, $k(x, y)$, in the first quadrant where $x \geq 0$ and $y \geq 0$. The equation is

$$(-\Delta_2 - k^2(x, y)) u_{sc}(x, y) = f(x, y), \quad (20)$$

where Δ_2 is the 2D Laplacian and the solution u_{sc} satisfies homogeneous boundary conditions $u_{sc}(x, 0) = 0$ for all $x \geq 0$ and $u_{sc}(0, y) = 0$ for all $y \geq 0$. On the other boundaries we have outgoing boundary conditions.

The right hand side $f(x, y)$ has a support that is limited to $[0, b]^2 \subset [0, L]^2 \subset \mathbb{R}_+^2$, i.e. $f(x, y) = 0$, for all $x \geq b$ or $y \geq b$.

The wave number $k(x, y)$ can be split in a constant part, k_0^2 and variable part $\chi(x, y)$. The variable part is also only non-zero on $[0, b]^2$

$$k^2(x, y) = \begin{cases} k_0^2 (1 + \chi(x, y)) & \text{if } x < b \text{ and } y < b, \\ k_0^2 & \text{if } x \geq b \text{ or } y \geq b. \end{cases} \quad (21)$$

We extend the domain with exterior complex scaling (ECS) absorbing boundary condition [13].

The wave function u_{sc} is discretized on the two dimensional mesh and can be represented as a matrix $\mathbf{A} \in \mathbb{C}^{n \times n}$. We can compute the singular decomposition of this matrix, $\mathbf{A} = \mathbf{U}\mathbf{\Sigma}\mathbf{V}^H$ where $\mathbf{U}, \mathbf{\Sigma}, \mathbf{V} \in \mathbb{C}^{n \times n}$ where $\mathbf{U}^H\mathbf{U} = \mathbf{I}$, $\mathbf{V}^H\mathbf{V} = \mathbf{I}$ and $\mathbf{\Sigma}$ is a diagonal matrix with the singular value σ_i on the diagonal.

The results are shown in Figure 3 and show that the singular values rapidly decrease. Thus the wave function can efficiently be approximated by a truncated representation,

$$\mathbf{A} \approx \sum_{i=1}^r \mathbf{u}_i \sigma_i \mathbf{v}_i^H, \quad (22)$$

where $\mathbf{u}_i \in \mathbb{C}^n$ are columns of \mathbf{U} and $\mathbf{v}_i \in \mathbb{C}^n$ are rows from \mathbf{V} and σ_i are largest r singular values. Thus \mathbf{A} is approximated by its low-rank representation with rank r . This truncated decomposition drops all contributions with $\sigma_i < \tau$ below a threshold τ , for example the expected discretisation error.

Figure 4 illustrates that a low-rank approximation to the wave function is sufficient to calculate an accurate approximation of the cross section.

3.2 Determining the low-rank components directly

In the example of the previous section, we have first calculated a matrix representation of the solution, $\mathbf{A} \in \mathbb{C}^{n \times n}$, and then approximated it by low-rank components. The aim is now to develop a method that calculates, directly, these components without first calculating the full solution \mathbf{A} . This approach avoids expensive calculations.

We start from the 2D Helmholtz equation as given in (20). In matrix form this is given by

$$-\mathbf{D}_{xx}\mathbf{A} - \mathbf{A}\mathbf{D}_{yy}^T - \mathbf{K} \circ \mathbf{A} = \mathbf{F}, \quad (23)$$

where $\mathbf{D}_{xx} \in \mathbb{C}^{n \times n}$ and $\mathbf{D}_{yy} \in \mathbb{C}^{n \times n}$ are sparse matrices that represent the discretization of the second derivatives, \mathbf{K} is the matrix that represents the space-dependent wave number, $k^2(x, y)$, on the grid and $\mathbf{A} \in \mathbb{C}^{n \times n}$ is the matrix that describes the unknown partial wave. The right hand side $\mathbf{F} \in \mathbb{C}^{n \times n}$ is given. The Hadamard product, \circ , multiplies the matrices point wise, element by element.

We now make the approximation $\mathbf{A} \approx \mathbf{U}\mathbf{V}^H$, with low-rank matrices $\mathbf{U} \in \mathbb{C}^{n \times r}$ and $\mathbf{V} \in \mathbb{C}^{n \times r}$ where $r \ll n$ and write

$$-\mathbf{D}_{xx}\mathbf{U}\mathbf{V}^H - \mathbf{U}\mathbf{V}^H\mathbf{D}_{yy} - \mathbf{K} \circ \mathbf{U}\mathbf{V}^H = \mathbf{F}. \quad (24)$$

We start with a guess for $\mathbf{V} \in \mathbb{C}^{n \times r}$ with orthogonal columns such that $\mathbf{V}^H\mathbf{V} = \mathbf{I}_r$. We can now multiply, (24), from the right, by \mathbf{V} and obtain

$$-\mathbf{D}_{xx}\mathbf{U}\mathbf{V}^H\mathbf{V} - \mathbf{U}\mathbf{V}^H\mathbf{D}_{yy}\mathbf{V} - (\mathbf{K} \circ \mathbf{U}\mathbf{V}^H)\mathbf{V} = \mathbf{F}\mathbf{V}. \quad (25)$$

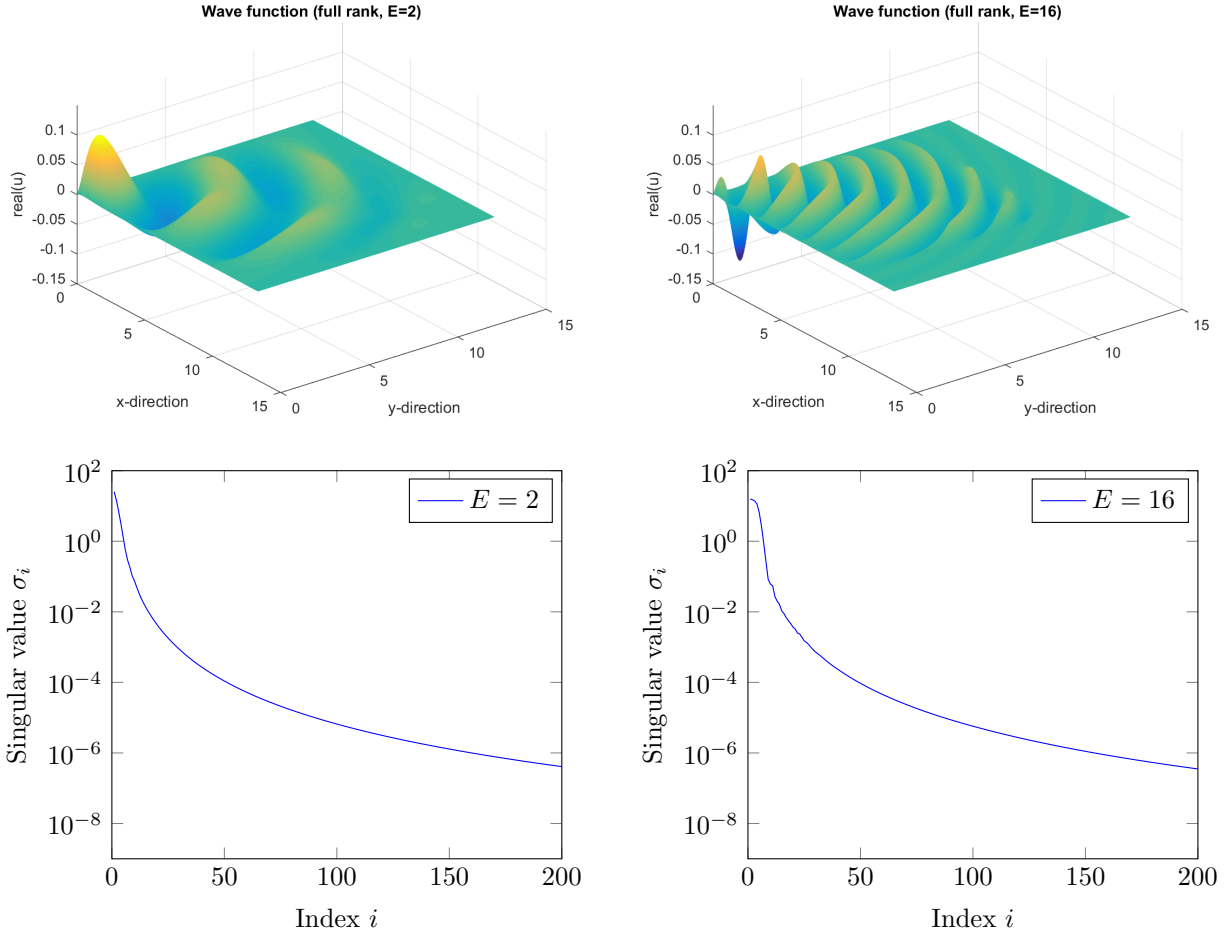


Figure 3: The top figures show the wave function for two different energies (i.e. $E = 2$ and $E = 16$). The singular values of the matrix-representation of the discretized functions are shown in the bottom figures. we show the solution of a 2D Helmholtz equation with a space-dependent wave number $k^2(x, y)$ given by $k^2(x, y) = E - e^{-|x-y|}$. The right hand side $f(x, y)$ on the finite domain $[0, b]^2$ is given by $f(x, y) = -e^{-x^2-y^2}$. Finite difference discretization is done on a uniform mesh with $M = 1000$ interior mesh points per dimension. At the boundaries $x = b$ and $y = b$ the domain is extended with exterior complex scaling under an angle $\frac{\pi}{6}$ where 33% additional discretization points are added, so $n = 1333$. We have $b = 10$.

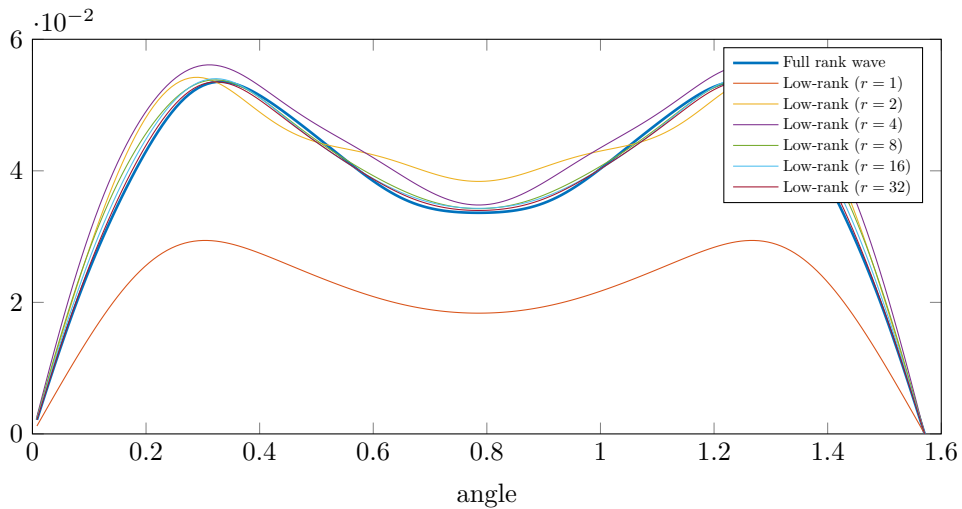


Figure 4: The cross section based on different low-rank approximations of the wave function.

Algorithm 1: Solve for the low-rank matrix decomposition of the solution $\mathbf{A} \approx \mathbf{U}\mathbf{V}^H$ of a 2D Helmholtz problem with space-dependent wave number.

```

1 Choose  $\mathbf{V} \in \mathbb{C}^{n \times r}$  as initial guess;
2  $[\mathbf{V}, \mathbf{R}] = \text{qr}[\mathbf{V}, 0]$ ;
3 while not converged do
4   Solve
    $\left[ -(\mathbf{I} \otimes \mathbf{D}_{xx}) - \left( (\mathbf{V}^H \mathbf{D}_{yy} \mathbf{V})^T \otimes \mathbf{I} \right) - (\mathbf{V}^T \otimes \mathbf{I}) \text{diag}(\text{vec}[\mathbf{K}]) \left( (\mathbf{V}^H)^T \otimes \mathbf{I} \right) \right] \text{vec}[\mathbf{U}] = \text{vec}[\mathbf{FV}];$ 
5    $[\mathbf{U}, \mathbf{R}] = \text{qr}[\mathbf{U}, 0]$ ;
6   Solve  $\left[ -(\mathbf{I} \otimes \mathbf{U}^H \mathbf{D}_{xx} \mathbf{U}) - (\mathbf{D}_{yy}^T \otimes \mathbf{I}) - (\mathbf{I} \otimes \mathbf{U}^H) \text{diag}(\text{vec}[\mathbf{K}]) (\mathbf{I} \otimes \mathbf{U}) \right] \text{vec}[\mathbf{V}^H] = \text{vec}[\mathbf{U}^H \mathbf{F}];$ 
7    $[\mathbf{V}, \mathbf{R}] = \text{qr}[\mathbf{V}, 0]$ ;
8 end
9  $\mathbf{A} = \mathbf{U}\mathbf{R}^H\mathbf{V}^H;$ 

```

where $\mathbf{U} \in \mathbb{C}^{n \times r}$ is now the remaining unknown. We use the vectorizing identities $\text{vec}[\mathbf{A} \circ \mathbf{B}] = \text{vec}[\mathbf{A}] \circ \text{vec}[\mathbf{B}]$ for $\mathbf{A}, \mathbf{B} \in \mathbb{C}^{l \times p}$ and $\text{vec}[\mathbf{AB}] = (\mathbf{I}_m \otimes \mathbf{A}) \text{vec}[\mathbf{B}] = (\mathbf{B}^T \otimes \mathbf{I}_k) \text{vec}[\mathbf{A}]$, for $\mathbf{A} \in \mathbb{C}^{k \times l}$ and $\mathbf{B} \in \mathbb{C}^{l \times m}$ and obtain

$$-(\mathbf{I}_r \otimes \mathbf{D}_{xx}) \text{vec}[\mathbf{U}] - \left((\mathbf{V}^H \mathbf{D}_{yy} \mathbf{V})^T \otimes \mathbf{I}_r \right) \text{vec}[\mathbf{U}] - \text{vec}[(\mathbf{K} \circ \mathbf{U}\mathbf{V}^H) \mathbf{V}] = \text{vec}[\mathbf{FV}]. \quad (26)$$

We can simplify the last term of the left hand side and write

$$\begin{aligned} \text{vec}[(\mathbf{K} \circ \mathbf{U}\mathbf{V}^H) \mathbf{V}] &= (\mathbf{V}^T \otimes \mathbf{I}) \text{vec}[\mathbf{K} \circ \mathbf{U}\mathbf{V}^H], \\ &= (\mathbf{V}^T \otimes \mathbf{I}) (\text{vec}[\mathbf{K}] \circ \text{vec}[\mathbf{U}\mathbf{V}^H]), \\ &= (\mathbf{V}^T \otimes \mathbf{I}) \text{diag}(\text{vec}[\mathbf{K}]) \text{vec}[\mathbf{U}\mathbf{V}^H], \\ &= (\mathbf{V}^T \otimes \mathbf{I}) \text{diag}(\text{vec}[\mathbf{K}]) \left((\mathbf{V}^H)^T \otimes \mathbf{I} \right) \text{vec}[\mathbf{U}]. \end{aligned} \quad (27)$$

This results in

$$\left[-(\mathbf{I} \otimes \mathbf{D}_{xx}) - \left((\mathbf{V}^H \mathbf{D}_{yy} \mathbf{V})^T \otimes \mathbf{I} \right) - (\mathbf{V}^T \otimes \mathbf{I}) \text{diag}(\text{vec}[\mathbf{K}]) \left((\mathbf{V}^H)^T \otimes \mathbf{I} \right) \right] \text{vec}[\mathbf{U}] = \text{vec}[\mathbf{FV}]. \quad (28)$$

This is a linear system for the remaining unknown columns of the matrix $\mathbf{U} \in \mathbb{C}^{n \times r}$.

In (22), we have approximated \mathbf{A} as $\mathbf{U}\mathbf{\Sigma}\mathbf{V}^H$ where $\mathbf{U}, \mathbf{V} \in \mathbb{C}^{n \times r}$ and $\mathbf{\Sigma} \in \mathbb{C}^{r \times r}$ are truncated matrices. With an orthogonal guess for \mathbf{V} , we solve for a \mathbf{U} in (28). Since we approximate \mathbf{A} now by the product $\mathbf{U}\mathbf{V}^H$, hence \mathbf{U} , solution of (28), includes the diagonal matrix with singular values.

We can now do a QR decomposition of \mathbf{U} to arrive at a guess for the orthogonal matrix \mathbf{U} .

The next step is to improve the guess for \mathbf{V} in a similar way. The equation (24) becomes, when we multiply from the left by \mathbf{U}^H ,

$$-\mathbf{U}^H \mathbf{D}_{xx} \mathbf{U}\mathbf{V}^H - \mathbf{U}^H \mathbf{U}\mathbf{V}^H \mathbf{D}_{yy} - \mathbf{U}^H (\mathbf{K} \circ \mathbf{U}\mathbf{V}^H) = \mathbf{U}^H \mathbf{F}. \quad (29)$$

Using the vectorizing identities this results in

$$\left[-(\mathbf{I} \otimes \mathbf{U}^H \mathbf{D}_{xx} \mathbf{U}) - (\mathbf{D}_{yy}^T \otimes \mathbf{I}) - (\mathbf{I} \otimes \mathbf{U}^H) \text{diag}(\text{vec}[\mathbf{K}]) (\mathbf{I} \otimes \mathbf{U}) \right] \text{vec}[\mathbf{V}^H] = \text{vec}[\mathbf{U}^H \mathbf{F}], \quad (30)$$

where we use that

$$\begin{aligned} \mathbf{U}^H (\mathbf{K} \circ \mathbf{U}\mathbf{V}^H) &= (\mathbf{I} \otimes \mathbf{U}^H) \text{vec}[\mathbf{K}] \circ \text{vec}[\mathbf{U}\mathbf{V}^H] \\ &= (\mathbf{I} \otimes \mathbf{U}^H) \text{diag}(\text{vec}[\mathbf{K}]) (\mathbf{I} \otimes \mathbf{U}) \text{vec}[\mathbf{V}^H]. \end{aligned} \quad (31)$$

Combining the equations (28) and (30) we can now propose an algorithm that updates \mathbf{U} and \mathbf{V} in an alternating way. The steps are described in the Algorithm 1.

3.3 Comparison between coupled channel and a low-rank decomposition

We now compare the coupled channel approach from section 2.4 with the low-rank approach from the previous section, Sec. 3.2. In the coupled channel calculation we use the eigenfunctions of one-particle subsystems as a basis for the expansion. After integration over one of the coordinates this results in a coupled set of one-dimensional equations. Let us illustrate that equation (28) and (30) reduce to the coupled channel equations when we choose the eigenfunctions, from (12) and (13), as columns for \mathbf{U} .

Let us take a look at the equation (30) and assume that $\mathbf{K} = E\mathbf{I} - V_1(\mathbf{x}) - V_2(\mathbf{y}) - V_{12}(\mathbf{x}, \mathbf{y})$ and that the columns of \mathbf{U} are the eigenstates of $-\mathbf{D}_{xx} + V_1(\mathbf{x})$. We can then write

$$-(\mathbf{I} \otimes \mathbf{U}^H) \text{diag}(\text{vec}[\mathbf{K}]) (\mathbf{I} \otimes \mathbf{U}) = -E\mathbf{I} \otimes \mathbf{I} + V_2(\mathbf{y}) \otimes \mathbf{I} + \mathbf{I} \otimes \mathbf{U}^H V_1(\mathbf{x}) \mathbf{U} + (\mathbf{I} \otimes \mathbf{U}^H) \text{diag}(\text{vec}[V_{12}(\mathbf{x}, \mathbf{y})]) (\mathbf{I} \otimes \mathbf{U}).$$

Then equation (30) becomes

$$[\mathbf{I} \otimes \mathbf{U}^H (-\mathbf{D}_{xx} + V_1(\mathbf{x})) \mathbf{U} + (-\mathbf{D}_{yy}^T + V_2(\mathbf{y}) - E\mathbf{I}) \otimes \mathbf{I} - (\mathbf{I} \otimes \mathbf{U}^H) \text{diag}(\text{vec}[V_{12}(\mathbf{x}, \mathbf{y})]) (\mathbf{I} \otimes \mathbf{U})] \text{vec}[\mathbf{V}^H] = \text{vec}[\mathbf{U}^H \mathbf{F}]$$

When we use that the columns of \mathbf{U} are eigenfunctions of $-\mathbf{D}_{xx} + V_1(\mathbf{x})$ with eigenvalues μ_i , equation (30) becomes

$$[\mathbf{I} \otimes \text{diag}(\boldsymbol{\mu}) + (-\mathbf{D}_{yy}^T + V_2(\mathbf{y}) - E\mathbf{I}) \otimes \mathbf{I} - (\mathbf{I} \otimes \mathbf{U}^H) \text{diag}(\text{vec}[V_{12}(\mathbf{x}, \mathbf{y})]) (\mathbf{I} \otimes \mathbf{U})] \text{vec}[\mathbf{V}^H] = \text{vec}[\mathbf{U}^H \mathbf{F}]. \quad (32)$$

The term $(\mathbf{I} \otimes \mathbf{U}^H) \text{diag}(\text{vec}[V_{12}(\mathbf{x}, \mathbf{y})]) (\mathbf{I} \otimes \mathbf{U})$ couples the columns of \mathbf{V} . It should be interpreted as a discretized version of $\int \phi_i^*(x) V(x, y) \phi_j(x) dx$, where we integrate over one of the coordinates. The columns of \mathbf{U} are the ϕ_i represented on a integration grid.

However, in general, the columns of \mathbf{U} are not eigenfunctions of the operator. The term $\mathbf{I} \otimes \text{diag}(\boldsymbol{\mu})$ then becomes a matrix that also couples the different components of \mathbf{V} .

In short, each iteration we are solving a generalized coupled channel equation.

3.4 Convergence with projection operators

We will now write both linear systems, (28) for $\text{vec}[\mathbf{U}]$, and, (30) for $\text{vec}[\mathbf{V}]$, as projection operators applied to the residual of the matrix equation, (23).

We denote by \mathbf{L} the discretized 2D Helmholtz operator on the full grid

$$\mathbf{L} = (\mathbf{I} \otimes (-\mathbf{D}_{xx})) + ((-\mathbf{D}_{yy}) \otimes \mathbf{I}) - \text{diag}(\text{vec}[\mathbf{K}]) (\mathbf{I} \otimes \mathbf{I}). \quad (33)$$

We can now explicitly write equation (28) in terms of projections and this linear operator:

$$(\mathbf{V}^T \otimes \mathbf{I}) \mathbf{L} (\bar{\mathbf{V}} \otimes \mathbf{I}) \text{vec}[\mathbf{U}] = (\mathbf{V}^T \otimes \mathbf{I}) \text{vec}[\mathbf{F}]. \quad (34)$$

The residual matrix, \mathbf{R} , is given by

$$\mathbf{R} = \mathbf{F} - (-\mathbf{D}_{xx}) \mathbf{U} \mathbf{V}^H - \mathbf{U} \mathbf{V}^H (-\mathbf{D}_{yy}) + \mathbf{K} \circ (\mathbf{U} \mathbf{V}^H). \quad (35)$$

In vector form this reads, using that \mathbf{U} is a solution of equation (34),

$$\begin{aligned} \text{vec}[\mathbf{R}] &= \text{vec}[\mathbf{F}] - (\bar{\mathbf{V}} \otimes (-\mathbf{D}_{xx}) + (-\mathbf{D}_{yy}^T) \bar{\mathbf{V}} \otimes \mathbf{I} - \text{diag}(\text{vec}[\mathbf{K}]) (\bar{\mathbf{V}} \otimes \mathbf{I})) \text{vec}[\mathbf{U}], \\ &= \left(\mathbf{I} - (\bar{\mathbf{V}} \otimes (-\mathbf{D}_{xx}) + (-\mathbf{D}_{yy}^T) \bar{\mathbf{V}} \otimes \mathbf{I} - \text{diag}(\text{vec}[\mathbf{K}]) (\bar{\mathbf{V}} \otimes \mathbf{I})) [(\mathbf{V}^T \otimes \mathbf{I}) \mathbf{L} (\bar{\mathbf{V}} \otimes \mathbf{I})]^{-1} (\mathbf{V}^T \otimes \mathbf{I}) \right) \text{vec}[\mathbf{F}] \\ &= \left(\mathbf{I} - \mathbf{L} (\bar{\mathbf{V}} \otimes \mathbf{I}) [(\mathbf{V}^T \otimes \mathbf{I}) \mathbf{L} (\bar{\mathbf{V}} \otimes \mathbf{I})]^{-1} (\mathbf{V}^T \otimes \mathbf{I}) \right) \text{vec}[\mathbf{F}] \\ &= P_{\mathbf{V}} \text{vec}[\mathbf{F}], \end{aligned} \quad (36)$$

where $P_{\mathbf{V}}$ is given by

$$\begin{aligned} P_{\mathbf{V}} &:= \mathbf{I} - \mathbf{L} (\bar{\mathbf{V}} \otimes \mathbf{I}) [(\mathbf{V}^T \otimes \mathbf{I}) \mathbf{L} (\bar{\mathbf{V}} \otimes \mathbf{I})]^{-1} (\mathbf{V}^T \otimes \mathbf{I}) \\ &:= \mathbf{I} - \mathbf{X}. \end{aligned} \quad (37)$$

The operator $P_{\mathbf{V}}$ is a projection operator. Indeed, observe that the terms between the two inverses cancel, in the next equation, against one of the inverse factors:

$$\begin{aligned} \mathbf{X}^2 &= \mathbf{L} (\bar{\mathbf{V}} \otimes \mathbf{I}) [(\mathbf{V}^T \otimes \mathbf{I}) \mathbf{L} (\bar{\mathbf{V}} \otimes \mathbf{I})]^{-1} (\mathbf{V}^T \otimes \mathbf{I}) \mathbf{L} (\bar{\mathbf{V}} \otimes \mathbf{I}) [(\mathbf{V}^T \otimes \mathbf{I}) \mathbf{L} (\bar{\mathbf{V}} \otimes \mathbf{I})]^{-1} (\mathbf{V}^T \otimes \mathbf{I}) \\ &= \mathbf{L} (\bar{\mathbf{V}} \otimes \mathbf{I}) [(\mathbf{V}^T \otimes \mathbf{I}) \mathbf{L} (\bar{\mathbf{V}} \otimes \mathbf{I})]^{-1} (\mathbf{V}^T \otimes \mathbf{I}) \\ &= \mathbf{X}. \end{aligned} \quad (38)$$

We then have that $P_{\mathbf{V}}^2 = (1 - \mathbf{X})(1 - \mathbf{X}) = 1 - 2\mathbf{X} + \mathbf{X}^2 = 1 - \mathbf{X} = P_{\mathbf{V}}$.

This projection operator removes all components from the residual matrix that can be corrected by the subspace spanned by \mathbf{V} . It is similar as a deflation operator, often used in preconditioning [7]. A similar derivation results in a projection operator P_U for the update of \mathbf{V} :

$$\begin{aligned} P_U &= \mathbf{I} - \mathbf{L} (\mathbf{I} \otimes \mathbf{U}) [(\mathbf{I} \otimes \mathbf{U}^H) \mathbf{L} (\mathbf{I} \otimes \mathbf{U})]^{-1} (\mathbf{I} \otimes \mathbf{U}^H) \\ &= \mathbf{I} - \mathbf{Y}. \end{aligned} \quad (39)$$

This is again a projection operator.

So, Algorithm 1 repeatedly projects the residual matrix, \mathbf{R} , on a subspace. Alternating between a subspace that is orthogonal to the subspace spanned by the columns of $\mathbf{V}^{(k)}$ at iteration k and a subspace that is orthogonal to the columns of $\mathbf{U}^{(k)}$ at iteration k . The residual matrix $\mathbf{R}^{(k)}$ after k iterations is the result of a series of projections

$$\mathbf{R}^{(k)} = P_{U^{(k)}} P_{V^{(k)}} P_{U^{(k-1)}} P_{V^{(k-1)}} \dots P_{U^{(0)}} P_{V^{(0)}} \mathbf{R}^{(0)}. \quad (40)$$

It is similar to the *method of Alternating Projections* [28] that goes back to Neumann [15], where a solution is projected on two alternating subspaces resulting in a solution that lies in the intersection between the two spaces. However, here the columns for $\mathbf{U}^{(k)}$ and $\mathbf{V}^{(k)}$ are changing each iteration.

However, when the rank of $\mathbf{U}^{(k)}$ and $\mathbf{V}^{(k)}$ is sufficiently large, the only intersection between the changing subspaces is the $\mathbf{0}$ matrix. So the residual converges to 0.

4 Solving for the low-rank tensor approximation of 3D Helmholtz equations

Algorithm 1, as introduced in section 3.2 for two dimensional problems, can be extended to higher dimensions. We illustrate now this extension for 3D Helmholtz problems. First, we will discuss the problem with a constant wave number and then extend the results to space-dependent wave numbers.

We solve the Helmholtz equation with a constant or space-dependent wave number, $k(x, y, z)$, in the first quadrant, where $x \geq 0, y \geq 0$ and $z \geq 0$. The equation is

$$(-\Delta_3 - k^2(x, y, z)) u_{sc}(x, y, z) = f(x, y, z), \quad (41)$$

where Δ_3 is the 3D Laplacian and the solution u_{sc} satisfies homogeneous boundary conditions $u_{sc}(0, y, z) = 0$ for all $y, z \geq 0$, $u_{sc}(x, 0, z) = 0$ for all $x, z \geq 0$ and $u_{sc}(x, y, 0) = 0$ for all $x, y \geq 0$. On the other boundaries we have outgoing boundary conditions.

The right hand side $f(x, y, z)$ has a support that is limited to $[0, b]^3 \subset [0, L]^3 \subset \mathbb{R}_+^3$, i.e. $f(x, y, z) = 0$, for all $x \geq b, y \geq b$ or $z \geq b$.

The wave number $k(x, y, z)$ can be split in a constant part, k_0^2 , and variable part $\chi(x, y, z)$. The variable part is also only non-zero on $[0, b]^3$

$$k^2(x, y, z) = \begin{cases} k_0^2 (1 + \chi(x, y, z)) & \text{if } x < b \text{ and } y < b \text{ and } z < b, \\ k_0^2 & \text{if } x \geq b \text{ or } y \geq b \text{ or } z \geq b. \end{cases} \quad (42)$$

We extend the domain with exterior complex scaling (ECS) absorbing boundary condition [13].

The wave function is discretized on a three dimensional mesh with $n_1 \times n_2 \times n_3$ unknowns and can be represented by a Tucker tensor decomposition [25] $\mathcal{M} \in \mathbb{C}^{n_1 \times n_2 \times n_3}$ with multi-linear rank $\mathbf{r} = (r_1, r_2, r_3)$:

$$\mathcal{M} = \mathcal{G} \times_1 \mathbf{U}_1 \times_2 \mathbf{U}_2 \times_3 \mathbf{U}_3 \in \mathbb{C}^{n_1 \times n_2 \times n_3}. \quad (43)$$

Here the tensor $\mathcal{G} \in \mathbb{C}^{r_1 \times r_2 \times r_3}$ is called the core tensor and the factor matrices $\mathbf{U}_i \in \mathbb{C}^{n_i \times r_i}$ have orthonormal columns for $i = 1, 2, 3$. Here r_i refers to the rank for each direction and n_i to the number of mesh points in each direction. So, to store this tensor only one core tensor and d factor matrices need to be stored, so the storage costs¹ scales $\mathcal{O}(r^d + dnr)$.

Let \mathcal{L} be the discretization of the three dimensional Helmholtz operator as given in (41). Observe that the operator \mathcal{L} can be written as a sum of Kronecker-products, where the matrix representation \mathbf{L} is of the following form

$$\mathbf{L} = -\mathbf{I} \otimes \mathbf{I} \otimes \mathbf{D}_{xx} - \mathbf{I} \otimes \mathbf{D}_{yy} \otimes \mathbf{I} - \mathbf{D}_{zz} \otimes \mathbf{I} \otimes \mathbf{I} - \text{diag}(\text{vec}[\mathcal{K}]) \mathbf{I} \otimes \mathbf{I} \otimes \mathbf{I}. \quad (44)$$

Here $\mathbf{D}_{xx} \in \mathbb{C}^{n_1 \times n_1}$, $\mathbf{D}_{yy} \in \mathbb{C}^{n_2 \times n_2}$ and $\mathbf{D}_{zz} \in \mathbb{C}^{n_3 \times n_3}$ are sparse matrices that represent the discretization of the second derivatives and \mathcal{K} is the tensor that represents the constant or space-dependent wave number, $k^2(x, y, z)$, discretized on the grid.

¹Here, we used the notation $r^d := \prod_{i=1}^d r_i$ and $r := \sqrt[d]{r^d}$, to deal with possible unequal number of discretization points n_i or ranks r_i in different directions for a Tucker tensor.

4.1 Helmholtz equation with constant wave number

First, consider the 3D Helmholtz problem with a constant wave number, so $k^2(x, y, z) \equiv k^2$. The application of the Helmholtz operator \mathcal{L} on tensor \mathcal{M} in Tucker tensor format is given by

$$\begin{aligned}
\mathcal{L}\mathcal{M} &= \mathcal{F} \\
\mathcal{L}\mathcal{M} &= -\mathcal{G} \times_1 \mathbf{D}_{xx} \mathbf{U}_1 \times_2 \mathbf{U}_2 \times_3 \mathbf{U}_3 \\
&\quad - \mathcal{G} \times_1 \mathbf{U}_1 \times_2 \mathbf{D}_{yy} \mathbf{U}_2 \times_3 \mathbf{U}_3 \\
&\quad - \mathcal{G} \times_1 \mathbf{U}_1 \times_2 \mathbf{U}_2 \times_3 \mathbf{D}_{zz} \mathbf{U}_3 \\
&\quad - k^2 \mathcal{G} \times_1 \mathbf{U}_1 \times_2 \mathbf{U}_2 \times_3 \mathbf{U}_3 \\
&= \mathcal{F}
\end{aligned} \tag{45}$$

where $\mathbf{U}_i^H \mathbf{U}_i = \mathbf{I}$ for $i = 1, 2, 3$ and \mathcal{F} is a tensor representation of the right hand side function f discretized on the grid.

4.1.1 Solving for product of basis functions and core terms (version 1)

Similar to the two dimensional case, we can derive equations to iteratively solve for the factors \mathbf{U}_1 , \mathbf{U}_2 and \mathbf{U}_3 . To derive the equations for \mathbf{U}_1 we start from (45) and multiply with \mathbf{U}_2 and \mathbf{U}_3 in the second and third direction, respectively:

$$\mathcal{L}\mathcal{M} \times_2 \mathbf{U}_2^H \times_3 \mathbf{U}_3^H = \mathcal{F} \times_2 \mathbf{U}_2^H \times_3 \mathbf{U}_3^H.$$

For a review of tensors, tensor decompositions and tensor operations like this tensor-times-matrix product denoted by the symbol \times_i we refer to [12].

Using explicitly the Tucker tensor representation for \mathcal{M} and that the columns of \mathbf{U}_i are orthonormal, the following expression is derived for the Helmholtz operator applied on a tensor in Tucker format

$$\mathcal{L}\mathcal{M} \times_2 \mathbf{U}_2^H \times_3 \mathbf{U}_3^H = \mathcal{G} \times_1 (-\mathbf{D}_{xx} - k^2 \mathbf{I}) \mathbf{U}_1 - \mathcal{G} \times_1 \mathbf{U}_1 \times_2 \mathbf{U}_2^H \mathbf{D}_{yy} \mathbf{U}_2 - \mathcal{G} \times_1 \mathbf{U}_1 \times_3 \mathbf{U}_3^H \mathbf{D}_{zz} \mathbf{U}_3.$$

Writing this tensor equation in the first unfolding leads to a matrix equation, recall the first unfolding is given by $\mathbf{M}_{(1)} = \overline{\mathbf{U}_1} \mathbf{G}_{(1)} (\mathbf{U}_3 \otimes \mathbf{U}_2)^H$, see also [12]:

$$\overline{(-\mathbf{D}_{xx} - k^2 \mathbf{I}) \mathbf{U}_1} \mathbf{G}_{(1)} - \overline{\mathbf{U}_1} \mathbf{G}_{(1)} (\mathbf{I} \otimes \mathbf{U}_2^H \mathbf{D}_{yy} \mathbf{U}_2)^H - \overline{\mathbf{U}_1} \mathbf{G}_{(1)} (\mathbf{U}_3^H \mathbf{D}_{zz} \mathbf{U}_3 \otimes \mathbf{I})^H = \mathbf{F}_{(1)} (\mathbf{U}_3 \otimes \mathbf{U}_2). \tag{46}$$

To solve this equation for \mathbf{U}_1 , it is written in vectorized form as

$$\left\{ \mathbf{I} \otimes \overline{(-\mathbf{D}_{xx} - k^2 \mathbf{I})} + \left[-\overline{(\mathbf{I} \otimes \mathbf{U}_2^H \mathbf{D}_{yy} \mathbf{U}_2)} - \overline{(\mathbf{U}_3^H \mathbf{D}_{zz} \mathbf{U}_3 \otimes \mathbf{I})} \right] \otimes \mathbf{I} \right\} \text{vec} \left[\underbrace{\overline{\mathbf{U}_1} \mathbf{G}_{(1)}}_{\mathbf{X}_1} \right] = \text{vec} [\mathbf{F}_{(1)} (\mathbf{U}_3 \otimes \mathbf{U}_2)]. \tag{47}$$

Observe that this is a square system with $n_1 \times r_2 r_3$ unknowns, where the solution in matrix form \mathbf{X}_1 could have, in general, a rank $r > r_1$. In a similar way, equations for \mathbf{U}_2 and \mathbf{U}_3 are derived by multiplying (45) with the other factor matrices in the appropriate directions:

$$\left\{ \mathbf{I} \otimes \overline{(-\mathbf{D}_{yy} - k^2 \mathbf{I})} + \left[-\overline{(\mathbf{I} \otimes \mathbf{U}_1^H \mathbf{D}_{xx} \mathbf{U}_1)} - \overline{(\mathbf{U}_3^H \mathbf{D}_{zz} \mathbf{U}_3 \otimes \mathbf{I})} \right] \otimes \mathbf{I} \right\} \text{vec} \left[\underbrace{\overline{\mathbf{U}_2} \mathbf{G}_{(2)}}_{\mathbf{X}_2} \right] = \text{vec} [\mathbf{F}_{(2)} (\mathbf{U}_3 \otimes \mathbf{U}_1)], \tag{48}$$

and

$$\left\{ \mathbf{I} \otimes \overline{(-\mathbf{D}_{zz} - k^2 \mathbf{I})} + \left[-\overline{(\mathbf{I} \otimes \mathbf{U}_1^H \mathbf{D}_{xx} \mathbf{U}_1)} - \overline{(\mathbf{U}_2^H \mathbf{D}_{yy} \mathbf{U}_2 \otimes \mathbf{I})} \right] \otimes \mathbf{I} \right\} \text{vec} \left[\underbrace{\overline{\mathbf{U}_3} \mathbf{G}_{(3)}}_{\mathbf{X}_3} \right] = \text{vec} [\mathbf{F}_{(3)} (\mathbf{U}_2 \otimes \mathbf{U}_1)]. \tag{49}$$

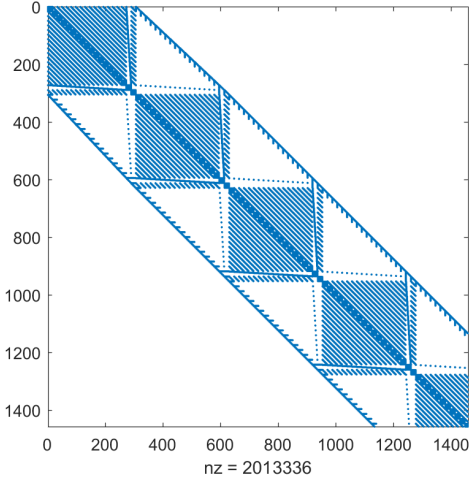
Alternating between solving for \mathbf{U}_1 , \mathbf{U}_2 and \mathbf{U}_3 using (47), (48) or (49) results in algorithm that approximates the low-rank solutions for three dimensional problems as given in (41). This algorithm is summarized in Algorithm 2. Also in the three dimensional case the orthogonality of the columns of \mathbf{U}_1 , \mathbf{U}_2 and \mathbf{U}_3 are maintained by additional QR factorizations. Observe that we solve for a large matrix $\mathbf{X}_i \in \mathbb{C}^{n_i \times r_1 r_2 r_3 / r_i}$. So, in general the rank of this matrix could be $\min(n_i, r_1 r_2 r_3 / r_i)$. But it is also known that $\mathbf{X}_i = \overline{\mathbf{U}_i} \mathbf{G}_{(i)}$ which

Algorithm 2: Solve for the low-rank tensor decomposition of the solution \mathcal{M} of a 3D Helmholtz with constant wave number (version 1).

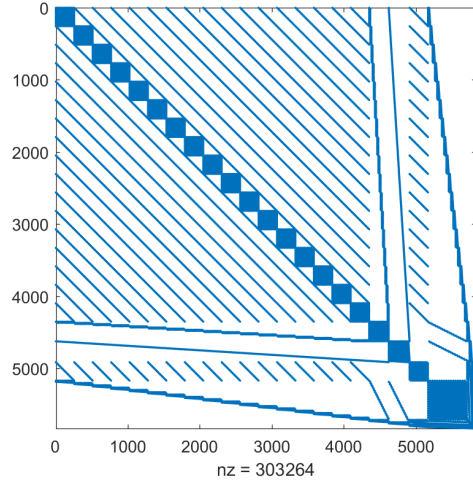
```

1  $[\mathcal{G}, \mathbf{U}_1, \mathbf{U}_2, \mathbf{U}_3] = \text{hosvd}(\text{initial guess});$ 
2 while not converged do
3   for  $i = 1, 2, 3$  do
4     Solve for  $\mathbf{X}_i = \overline{\mathbf{U}}_i \mathbf{G}_{(i)} \in \mathbb{C}^{n \times r^{d-1}}$  using (47), (48) or (49);
5      $\overline{\mathbf{U}}_i \mathbf{G}_{(i)} = \text{qr}[\mathbf{X}_i(:, 1:r_i), 0];$ 
6   end
7 end
8  $\mathcal{G} = \text{reconstruct}[\mathbf{G}_{(i)}, i];$ 
9  $\mathcal{M} = \mathcal{G} \times_1 \mathbf{U}_1 \times_2 \mathbf{U}_2 \times_3 \mathbf{U}_3;$ 

```



(a) Sparsity pattern of the top of the symmetric reverse Cuthill-McKee permutation of the system matrix to solve for \mathbf{X}_i using (47). Note: only the first 4.5 of the 168 blocks are shown.



(b) Sparsity pattern of the symmetric reverse Cuthill-McKee permutation of the system matrix to solve for $\mathbf{G}_{(1)}$ using (53).

Figure 5: Sparsity patterns of the symmetric reverse Cuthill-McKee permutation of certain system matrices ($d = 3, n = 168, r = 18$).

leads to the fact that the rank of \mathbf{X}_i should be at most r_i . Selecting the first r_i columns of \mathbf{X}_i and computing its QR decomposition is sufficient to derive a new orthonormal basis as factor matrix $\overline{\mathbf{U}}_i$.

Finally, observe that solving for \mathbf{X}_i using (47), (48) or (49) is computationally not efficient. In all iterations, we solve for a total of dnr^{d-1} unknowns, while there are only $r^d + dnr$ unknowns in the Tucker tensor factorization. Furthermore, solving equations (47), (48) and (49) is also expensive. Indeed, computing a symmetric reverse Cuthill-McKee permutation of the system matrix one observes a matrix with a bandwidth $\mathcal{O}(r^{d-1})$. For example when $d = 3, n_i = n = 168, r_i = r = 18$ one obtains the sparsity pattern on the diagonal of the matrix as shown in Figure 5a. So solving a system as given in (47), (48) or (49) has a computational cost of $\mathcal{O}(nr^{2(d-1)})$.

4.1.2 Solving for the basis functions and the core tensor separately (version 2)

To circumvent solving the large systems in (47), (48) and (49), we can pre-compute the QR factorization of the unfolding of the core tensor, $\mathbf{G}_{(i)}$, and project the equations onto the obtained \mathbf{Q}_i . Indeed, this will further reduce the number of unknowns in these linear systems to exactly the number of unknowns that are needed for the factor matrices $\overline{\mathbf{U}}_i$, for $i = 1, 2, 3$.

Let us discuss the details. We start again from equation (46) and use the QR factorization of $\mathbf{G}_{(1)}^H$, $\mathbf{Q}_1 \mathbf{R}_1^H = \text{qr}[\mathbf{G}_{(1)}^H]$. This yields

$$\overline{(-\mathbf{D}_{xx} - k^2 \mathbf{I}) \mathbf{U}_1 \mathbf{R}_1 \mathbf{Q}_1^H - \overline{\mathbf{U}}_1 \mathbf{R}_1 \mathbf{Q}_1^H (I \otimes \mathbf{U}_2^H \mathbf{D}_{yy} \mathbf{U}_2)^H - \overline{\mathbf{U}}_1 \mathbf{R}_1 \mathbf{Q}_1^H (\mathbf{U}_3^H \mathbf{D}_{zz} \mathbf{U}_3 \otimes I)^H = \mathbf{F}_{(1)} (\mathbf{U}_3 \otimes \mathbf{U}_2)}.$$

Algorithm 3: Solve for the low-rank tensor decomposition of the solution \mathcal{M} of a 3D Helmholtz problem with constant wave number (version 2).

```

1  $[\mathcal{G}, \mathbf{U}_1, \mathbf{U}_2, \mathbf{U}_3] = \text{hosvd}(\text{initial guess});$ 
2 while not converged do
3   for  $i = 1, 2, 3$  do
4      $\mathbf{Q}_i \tilde{\mathbf{R}} = \text{qr} [\mathbf{G}_{(i)}^H, 0];$ 
5     Solve for  $\mathbf{X}_i = \overline{\mathbf{U}_i} \mathbf{R}_i \in \mathbb{C}^{n_i \times r_i}$  using (50), (51) or (52);
6      $\overline{\mathbf{U}_i} \mathbf{R}_i = \text{qr} [\mathbf{X}_i, 0];$ 
7      $\mathcal{G} = \text{reconstruct} [\mathbf{R}_i \mathbf{Q}_i^H, i];$ 
8   end
9 end
10 Solve for  $\mathbf{G}_{(1)} \in \mathbb{C}^{r_1 \times r_2 r_3}$  using (53);
11  $\mathcal{G} = \text{reconstruct} [\mathbf{G}_{(1)}, 1];$ 
12  $\mathcal{M} = \mathcal{G} \times_1 \mathbf{U}_1 \times_2 \mathbf{U}_2 \times_3 \mathbf{U}_3;$ 

```

Post multiplication of this equation by \mathbf{Q}_1 yields

$$\overline{(-D_{xx} - k^2 \mathbf{I}) \mathbf{U}_1 \mathbf{R}_1} - \overline{\mathbf{U}_1 \mathbf{R}_1 \mathbf{Q}_1^H} (\mathbf{I} \otimes \mathbf{U}_2^H \mathbf{D}_{yy} \mathbf{U}_2)^H \mathbf{Q}_1 - \overline{\mathbf{U}_1 \mathbf{R}_1 \mathbf{Q}_1^H} (\mathbf{U}_3^H \mathbf{D}_{zz} \mathbf{U}_3 \otimes \mathbf{I})^H \mathbf{Q}_1 = \mathbf{F}_{(1)} (\mathbf{U}_3 \otimes \mathbf{U}_2) \mathbf{Q}_1.$$

To solve this equation for \mathbf{U}_1 , it is written in vectorized form as

$$\left\{ \mathbf{I} \otimes \overline{(-D_{xx} - k^2 \mathbf{I})} + \mathbf{Q}_1^T \left[-\overline{(\mathbf{I} \otimes \mathbf{U}_2^H \mathbf{D}_{yy} \mathbf{U}_2)} - \overline{(\mathbf{U}_3^H \mathbf{D}_{zz} \mathbf{U}_3 \otimes \mathbf{I})} \right] \overline{\mathbf{Q}_1} \otimes \mathbf{I} \right\} \text{vec} \left[\underbrace{\overline{\mathbf{U}_1 \mathbf{R}_1}}_{\mathbf{X}_1} \right] = \text{vec} [\mathbf{F}_{(1)} (\mathbf{U}_3 \otimes \mathbf{U}_2) \mathbf{Q}_1]. \quad (50)$$

In a similar way, the update equations for \mathbf{U}_2 and \mathbf{U}_3 are derived by multiplying (45) with the other factor matrices in the appropriate dimensions and using the QR factorizations of $\mathbf{G}_{(i)}^H$:

$$\left\{ \mathbf{I} \otimes \overline{(-D_{yy} - k^2 \mathbf{I})} + \mathbf{Q}_2^T \left[-\overline{(\mathbf{I} \otimes \mathbf{U}_1^H \mathbf{D}_{xx} \mathbf{U}_1)} - \overline{(\mathbf{U}_3^H \mathbf{D}_{zz} \mathbf{U}_3 \otimes \mathbf{I})} \right] \overline{\mathbf{Q}_2} \otimes \mathbf{I} \right\} \text{vec} \left[\underbrace{\overline{\mathbf{U}_2 \mathbf{R}_2}}_{\mathbf{X}_2} \right] = \text{vec} [\mathbf{F}_{(2)} (\mathbf{U}_3 \otimes \mathbf{U}_1) \mathbf{Q}_2]. \quad (51)$$

and

$$\left\{ \mathbf{I} \otimes \overline{(-D_{zz} - k^2 \mathbf{I})} + \mathbf{Q}_3^T \left[-\overline{(\mathbf{I} \otimes \mathbf{U}_1^H \mathbf{D}_{xx} \mathbf{U}_1)} - \overline{(\mathbf{U}_2^H \mathbf{D}_{yy} \mathbf{U}_2 \otimes \mathbf{I})} \right] \overline{\mathbf{Q}_3} \otimes \mathbf{I} \right\} \text{vec} \left[\underbrace{\overline{\mathbf{U}_3 \mathbf{R}_3}}_{\mathbf{X}_3} \right] = \text{vec} [\mathbf{F}_{(3)} (\mathbf{U}_2 \otimes \mathbf{U}_1) \mathbf{Q}_3]. \quad (52)$$

All these equations are cheap to solve. Indeed, $\text{vec} [\overline{\mathbf{U}_i \mathbf{R}_i}]$ has length $n_i r_i$. Computing a symmetric reverse Cuthill-McKee permutation of these system matrices one observes a matrix with a bandwidth $\mathcal{O}(r)$, so solving these equations has a computational cost $\mathcal{O}(nr^2)$.

Of course, this only updates the factor matrices as basis vectors in each direction. As a single final step, we still have to compute the core tensor \mathcal{G} . This will be the computationally most expensive part.

Core tensor \mathcal{G} can be obtained by multiplying (45) with all the d factor matrices in the matching directions. Unfolding this equation in a certain direction (eg. the first folding) leads again to a matrix equation. In vectorized form, it is given by

$$\left\{ \mathbf{I} \otimes \overline{\mathbf{U}_1^H (-D_{xx} - k^2 \mathbf{I}) \mathbf{U}_1} + \left[-\overline{(\mathbf{I} \otimes \mathbf{U}_2^H \mathbf{D}_{yy} \mathbf{U}_2)} - \overline{(\mathbf{U}_3^H \mathbf{D}_{zz} \mathbf{U}_3 \otimes \mathbf{I})} \right] \otimes \mathbf{I} \right\} \text{vec} [\mathbf{G}_{(1)}] = \text{vec} [\mathbf{U}_1^T \mathbf{F}_{(1)} (\mathbf{U}_3 \otimes \mathbf{U}_2)]. \quad (53)$$

Indeed, considering again an example where $d = 3, n_i = n = 168, r_i = r = 18$ one obtains a matrix with a sparsity pattern that is shown in Figure 5b. Hence, this matrix has not a limited bandwidth anymore. It coupled all functions to all other functions. Although this equation has to be solved only once in the algorithm, when the rank increases, it will rapidly dominate the computational cost of this algorithm.

4.1.3 Efficient combination of version 1 and version 2 into new algorithm (version 3)

In the first version of the algorithm, (see section 4.1.1), an update for $\mathbf{G}_{(i)}$ is computed for each direction in each iteration. This leads to a too expensive algorithm. Then we changed the algorithm such that the costs for

Algorithm 4: Solve for the low-rank tensor decomposition of the solution \mathcal{M} of a 3D Helmholtz problem with constant wave number (version 3).

```

1  $[\mathcal{G}, \mathbf{U}_1, \mathbf{U}_2, \mathbf{U}_3] = \text{hosvd}(\text{initial guess});$ 
2 while not converged do
3   for  $i = 1, 2$  do
4      $\mathbf{Q}_i \tilde{\mathbf{R}} = \text{qr} [\mathbf{G}_{(i)}^H, 0];$ 
5     Solve for  $\mathbf{X}_i = \overline{\mathbf{U}}_i \mathbf{R}_i \in \mathbb{C}^{n_i \times r_i}$  using (50) or (51);
6      $\overline{\mathbf{U}}_i \mathbf{R}_i = \text{qr} [\mathbf{X}_i, 0];$ 
7      $\mathcal{G} = \text{reconstruct} [\mathbf{R}_i \mathbf{Q}_i^H, i];$ 
8   end
9   Solve for  $\mathbf{X}_3 = \overline{\mathbf{U}}_3 \mathbf{G}_{(3)} \in \mathbb{C}^{n_3 \times r^{d-1}}$  using (49);
10   $\overline{\mathbf{U}}_3 \mathbf{G}_{(3)} = \text{qr} [\mathbf{X}_3, 0];$ 
11   $\mathcal{G} = \text{reconstruct} [\mathbf{G}_{(3)}, 3];$ 
12 end
13  $\mathcal{M} = \mathcal{G} \times_1 \mathbf{U}_1 \times_2 \mathbf{U}_2 \times_3 \mathbf{U}_3;$ 

```

the updates in each direction is reduced, (see section 4.1.2). But, in that version almost all information for a full update of core tensor \mathcal{G} is lost. Therefore a final, but potential too expensive, equation needs to be solved. Observe that the expensive computation for the full core tensor, in version 2, can now be replaced by a single solve per iteration as done in version 1. This leads to a third version of the algorithm. It avoids repeatedly solving the large systems (like version 1) and it does not solve too expensive systems (like version 2). The computational complexity of this algorithm is equal to the complexity of version 1, so $\mathcal{O}(nr^{2(d-1)})$. Furthermore, the systems that need to be solved, each iteration, have exactly the same number of unknowns as the representation of the tensor in low-rank Tucker tensor format. In summary, this final version of the algorithm is given by Algorithm 4.

4.1.4 Numerical comparison of three versions for 3D Helmholtz equation

Consider a three dimensional domain $\Omega = [-10, 10]^3$ that is discretized with $M = 100$ equidistant mesh points per direction in the interior of the domain. The domain is extended with exterior complex scaling to implement the absorbing boundary conditions. Hence, in total there are $n = n_x = n_y = n_z = 168$ unknowns per direction. As constant wave number we use $\omega = 2$ and a right hand side $f(x, y, z) = -e^{-x^2 - y^2 - z^2}$. By symmetry, we expect a low rank factorization with a equal low-rank in each direction, so we fix $r = r_x = r_y = r_z$.

The convergence of the residuals of the three versions are given in the left column of Figure 6. It is clear that all three versions converge to a good low-rank approximation of the full solution. By increasing the maximal attainable rank r , a better low-rank solution is obtained, as expected. Remarkably, for $r = 30$, in version 2, the final residual is larger than the residuals obtained by both other algorithms while the compute-time for version 2 is larger than the other algorithms.

The compute-time for the most time-consuming parts in the different versions of the algorithm can be measured as a function of the maximal attainable rank r . For the three versions of the algorithm the runtimes are shown in the right column of Figure 6. For all parts the expected and measured dependence on the rank r are given. For all versions of the algorithm 10 iterations are applied.

Comparing the total runtime for the three different versions one obtains results as shown in Figure 7. Indeed, as expected version 3 is approximately 3 times faster than version 1 and the runtime scales similar in rank r . Further, for small rank r version 2 is faster than both other versions. But when the rank increases the expensive solve for the core tensor \mathcal{G} starts to dominate the runtime. The total runtime will increase dramatically.

4.2 Projection operator for constant wave number

Also in three dimensions we can write the linear systems (47) for \mathbf{U}_1 , (48) for \mathbf{U}_2 and (49) for \mathbf{U}_3 as projection operators applied to the residual of the tensor equation, (45).

Consider a tensor \mathcal{M} in Tucker format and factorized as $\mathcal{M} = \mathcal{G} \times_1 \mathbf{U}_1 \times_2 \mathbf{U}_2 \times_3 \mathbf{U}_3$, with unknowns $\mathcal{G}, \mathbf{U}_1, \mathbf{U}_2$ and \mathbf{U}_3 . Discretization of (41) leads to a linear operator \mathcal{L} applied on tensors. Its matrix representation \mathbf{L} has a sum of Kronecker products structure, as given in (44).

Solving for an unknown factors $\mathbf{U}_1, \mathbf{U}_2$ or \mathbf{U}_3 (and the core-tensor \mathcal{G}) using (47), (48) or (49) can be interpreted

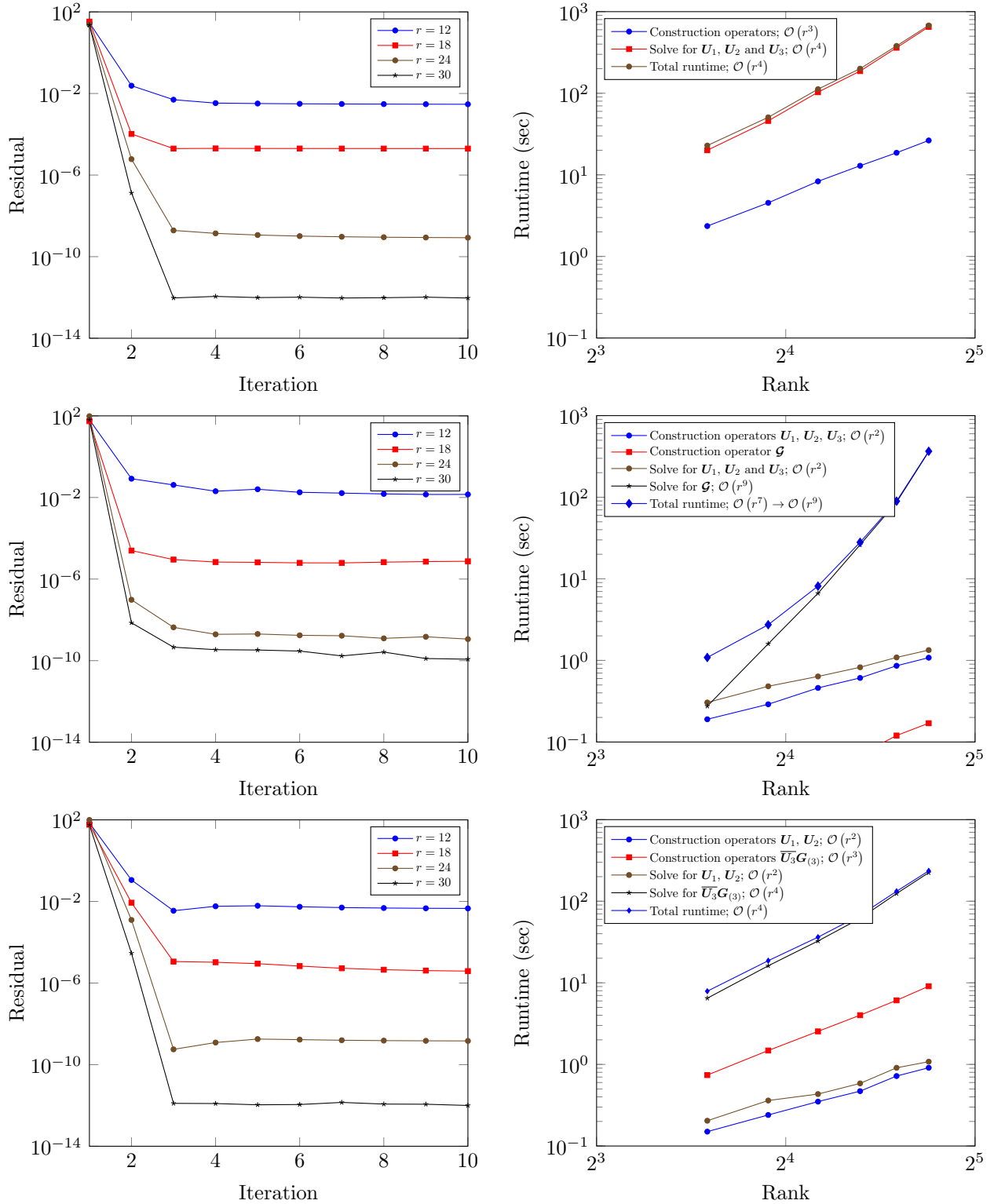


Figure 6: Left: Plot of residual per iteration for constant wave number in 3D Helmholtz problem. Right: Plot of runtime of most time consuming parts for constant wave number in 3D Helmholtz problem. Both problems have $M = 100$. Top: Algorithm 2 (version 1), middle: Algorithm 3 (version 2), bottom: Algorithm 4 (version 3).

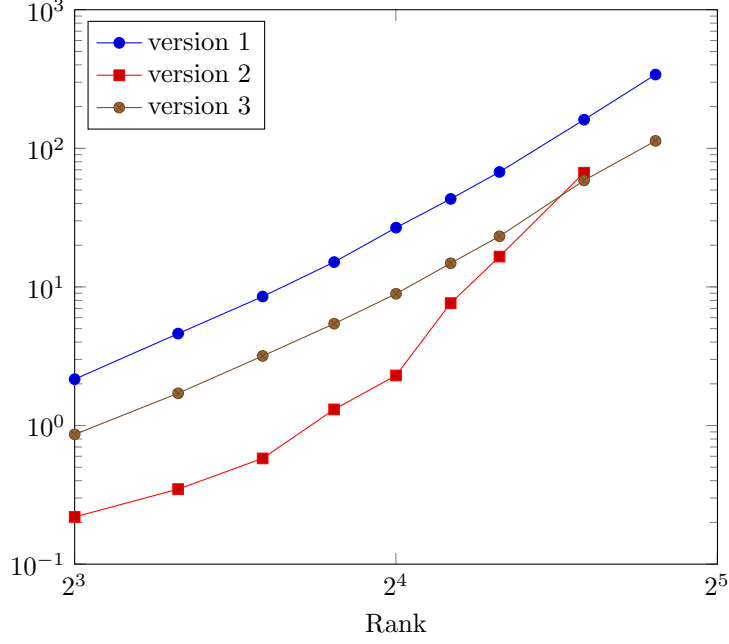


Figure 7: Plot of runtime for 4 iteration with constant wavenumber in 3D using the three different algorithms ($M = 100$)

as a projection operator applied on the residual. For example, (47) can be interpreted as

$$\overline{(\mathbf{U}_3^H \otimes \mathbf{U}_2^H \otimes \mathbf{I}) \mathbf{L}(\mathbf{U}_3 \otimes \mathbf{U}_2 \otimes \mathbf{I})} \text{vec} [\overline{\mathbf{U}_1 \mathbf{G}_{(1)}}] = (\mathbf{U}_3^T \otimes \mathbf{U}_2^T \otimes \mathbf{I}) \text{vec} [\mathbf{F}_{(1)}]. \quad (54)$$

The residual, in tensor format, is given by

$$\begin{aligned} \mathcal{R} &= \mathcal{F} - \mathcal{L}\mathcal{M}, \\ &= \mathcal{F} - \mathcal{G} \times_1 (-\mathbf{D}_{xx} - k^2 \mathbf{I}) \mathbf{U}_1 \times_2 \mathbf{U}_2 \times_3 \mathbf{U}_3 + \mathcal{G} \times_1 \mathbf{U}_1 \times_2 \mathbf{D}_{yy} \mathbf{U}_2 \times_3 \mathbf{U}_3 + \mathcal{G} \times_1 \mathbf{U}_1 \times_2 \mathbf{U}_2 \times_3 \mathbf{D}_{zz} \mathbf{U}_3. \end{aligned} \quad (55)$$

Writing this tensor equation in the first unfolding leads to the following matrix equation

$$\mathbf{R}_{(1)} = \mathbf{F}_{(1)} - \overline{(-\mathbf{D}_{xx} - k^2 \mathbf{I}) \mathbf{U}_1 \mathbf{G}_{(1)}} (\mathbf{U}_3 \otimes \mathbf{U}_2)^H + \overline{\mathbf{U}_1 \mathbf{G}_{(1)}} (\mathbf{U}_3 \otimes \mathbf{D}_{yy} \mathbf{U}_2)^H + \overline{\mathbf{U}_1 \mathbf{G}_{(1)}} (\mathbf{D}_{zz} \mathbf{U}_3 \otimes \mathbf{U}_2)^H, \quad (56)$$

which can be vectorized as

$$\begin{aligned} \text{vec} [\mathbf{R}_{(1)}] &= \text{vec} [\mathbf{F}_{(1)}] - \left(\overline{(\mathbf{U}_3 \otimes \mathbf{U}_2 \otimes (-\mathbf{D}_{xx} - k^2 \mathbf{I}))} - \overline{(\mathbf{U}_3 \otimes \mathbf{D}_{yy} \mathbf{U}_2 \otimes \mathbf{I})} - \overline{(\mathbf{D}_{zz} \mathbf{U}_3 \otimes \mathbf{U}_2 \otimes \mathbf{I})} \right) \text{vec} [\overline{\mathbf{U}_1 \mathbf{G}_{(1)}}] \\ &= \text{vec} [\mathbf{F}_{(1)}] - \overline{\mathbf{L}(\mathbf{U}_3 \otimes \mathbf{U}_2 \otimes \mathbf{I})} \text{vec} [\overline{\mathbf{U}_1 \mathbf{G}_{(1)}}] \\ &= \text{vec} [\mathbf{F}_{(1)}] - \overline{\mathbf{L}(\mathbf{U}_3 \otimes \mathbf{U}_2 \otimes \mathbf{I})} \left[\overline{(\mathbf{U}_3^H \otimes \mathbf{U}_2^H \otimes \mathbf{I}) \mathbf{L}(\mathbf{U}_3 \otimes \mathbf{U}_2 \otimes \mathbf{I})} \right]^{-1} (\mathbf{U}_3^T \otimes \mathbf{U}_2^T \otimes \mathbf{I}) \text{vec} [\mathbf{F}_{(1)}] \\ &= P_{23} \text{vec} [\mathbf{F}_{(1)}], \end{aligned} \quad (57)$$

where operator P_{23} is given by

$$\begin{aligned} P_{23} &= \mathbf{I} - \overline{\mathbf{L}(\mathbf{U}_3 \otimes \mathbf{U}_2 \otimes \mathbf{I})} \left[\overline{(\mathbf{U}_3^H \otimes \mathbf{U}_2^H \otimes \mathbf{I}) \mathbf{L}(\mathbf{U}_3 \otimes \mathbf{U}_2 \otimes \mathbf{I})} \right]^{-1} (\mathbf{U}_3^T \otimes \mathbf{U}_2^T \otimes \mathbf{I}) \\ &= \mathbf{I} - \mathbf{X}. \end{aligned} \quad (58)$$

This operator P_{23} is indeed a projection operator. Observe that the terms between the two inverses cancel against one of the inverse factors:

$$\begin{aligned} \mathbf{X}^2 &= \overline{\mathbf{L}(\mathbf{U}_3 \otimes \mathbf{U}_2 \otimes \mathbf{I})} \left[\overline{(\mathbf{U}_3^H \otimes \mathbf{U}_2^H \otimes \mathbf{I}) \mathbf{L}(\mathbf{U}_3 \otimes \mathbf{U}_2 \otimes \mathbf{I})} \right]^{-1} (\mathbf{U}_3^T \otimes \mathbf{U}_2^T \otimes \mathbf{I}) \overline{\mathbf{L}(\mathbf{U}_3 \otimes \mathbf{U}_2 \otimes \mathbf{I})} \left[\overline{(\mathbf{U}_3^H \otimes \mathbf{U}_2^H \otimes \mathbf{I}) \mathbf{L}(\mathbf{U}_3 \otimes \mathbf{U}_2 \otimes \mathbf{I})} \right]^{-1} \\ &= \overline{\mathbf{L}(\mathbf{U}_3 \otimes \mathbf{U}_2 \otimes \mathbf{I})} \left[\overline{(\mathbf{U}_3^H \otimes \mathbf{U}_2^H \otimes \mathbf{I}) \mathbf{L}(\mathbf{U}_3 \otimes \mathbf{U}_2 \otimes \mathbf{I})} \right]^{-1} (\mathbf{U}_3^T \otimes \mathbf{U}_2^T \otimes \mathbf{I}) \\ &= \mathbf{X}. \end{aligned}$$

This operator is a natural extension to higher dimensions of the two dimensional operators as derived in section 3.4.

A similar derivation results in projection operators P_{13} and P_{12} for the updates in \mathbf{U}_2 and \mathbf{U}_3 , respectively.

$$\begin{aligned} P_{23} &= \mathbf{I} - \overline{\mathbf{L}(\mathbf{U}_3 \otimes \mathbf{U}_2 \otimes \mathbf{I})} \left[\overline{(\mathbf{U}_3^{\text{H}} \otimes \mathbf{U}_2^{\text{H}} \otimes \mathbf{I}) \mathbf{L}(\mathbf{U}_3 \otimes \mathbf{U}_2 \otimes \mathbf{I})} \right]^{-1} (\mathbf{U}_3^{\text{T}} \otimes \mathbf{U}_2^{\text{T}} \otimes \mathbf{I}), \\ P_{13} &= \mathbf{I} - \overline{\mathbf{L}(\mathbf{U}_3 \otimes \mathbf{I} \otimes \mathbf{U}_1)} \left[\overline{(\mathbf{U}_3^{\text{H}} \otimes \mathbf{I} \otimes \mathbf{U}_1^{\text{H}}) \mathbf{L}(\mathbf{U}_3 \otimes \mathbf{I} \otimes \mathbf{U}_1)} \right]^{-1} (\mathbf{U}_3^{\text{T}} \otimes \mathbf{I} \otimes \mathbf{U}_1^{\text{T}}), \\ P_{12} &= \mathbf{I} - \overline{\mathbf{L}(\mathbf{I} \otimes \mathbf{U}_2 \otimes \mathbf{U}_1)} \left[\overline{(\mathbf{I} \otimes \mathbf{U}_2^{\text{H}} \otimes \mathbf{U}_1^{\text{H}}) \mathbf{L}(\mathbf{I} \otimes \mathbf{U}_2 \otimes \mathbf{U}_1)} \right]^{-1} (\mathbf{I} \otimes \mathbf{U}_2^{\text{T}} \otimes \mathbf{U}_1^{\text{T}}). \end{aligned} \quad (59)$$

The successive application of these projection operators on the residual results in an updated residual that lies in the intersection of all subspaces.

4.3 Helmholtz equation with space-dependent wave number

The presented algorithms with constant wave number can be extended to space-dependent wave numbers. So, lets consider a 3D Helmholtz problem where $\mathcal{K} = k^2(x, y, z)$ represents the space-dependent wave number on the discretized mesh.

Further, we assume that a Canonical Polyadic decomposition of the space-dependent wave number tensor \mathcal{K} is known, i.e.

$$\mathcal{K} = \sum_{i=1}^s \sigma_i \left(\mathbf{v}_i^{(1)} \circ \mathbf{v}_i^{(2)} \circ \dots \circ \mathbf{v}_i^{(d)} \right), \quad (60)$$

where $s \in \mathbb{N}_+$ is the CP-rank of \mathcal{K} and $\mathbf{v}_i^{(j)} \in \mathbb{C}^{n_j}$ for $i = 1, 2, \dots, s; j = 1, 2, \dots, d$ are vectors. Further, σ_i is a tensor generalization of a singular value and \circ denotes the vector outer product.

The application of the space-dependent Helmholtz operator \mathcal{L} on tensor \mathcal{M} is given by

$$\begin{aligned} \mathcal{L}\mathcal{M} &= \mathcal{F} \\ \mathcal{L}\mathcal{M} &= -\mathcal{G} \times_1 \mathbf{D}_{xx} \mathbf{U}_1 \times_2 \mathbf{U}_2 \times_3 \mathbf{U}_3 \\ &\quad - \mathcal{G} \times_1 \mathbf{U}_1 \times_2 \mathbf{D}_{yy} \mathbf{U}_2 \times_3 \mathbf{U}_3 \\ &\quad - \mathcal{G} \times_1 \mathbf{U}_1 \times_2 \mathbf{U}_2 \times_3 \mathbf{D}_{zz} \mathbf{U}_3 \\ &\quad - \mathcal{K} \circ (\mathcal{G} \times_1 \mathbf{U}_1 \times_2 \mathbf{U}_2 \times_3 \mathbf{U}_3) \\ &= \mathcal{F}, \end{aligned} \quad (61)$$

where $\mathbf{U}_i^{\text{H}} \mathbf{U}_i = \mathbf{I}$ for $i = 1, 2, 3$ and \mathcal{F} is a tensor representation of the right hand side function f discretized on the used grid. Here \circ denotes the Hadamard product for tensors.

In a similar way as in the three dimensional constant wave number case, we can derive equations to iteratively solve for the factors \mathbf{U}_1 , \mathbf{U}_2 and \mathbf{U}_3 . We start from (61) and multiply with \mathbf{U}_2 and \mathbf{U}_3 in the second and third direction, respectively. Using that the columns of \mathbf{U}_i are orthonormal, the following expression is derived:

$$\mathcal{L}\mathcal{M} \times_2 \mathbf{U}_2^{\text{H}} \times_3 \mathbf{U}_3^{\text{H}} = -\mathcal{G} \times_1 \mathbf{D}_{xx} - \mathcal{G} \times_1 \mathbf{U}_1 \times_2 \mathbf{U}_2^{\text{H}} \mathbf{D}_{yy} \mathbf{U}_2 - \mathcal{G} \times_1 \mathbf{U}_1 \times_3 \mathbf{U}_3^{\text{H}} \mathbf{D}_{zz} \mathbf{U}_3 - [\mathcal{K} \circ (\mathcal{G} \times_1 \mathbf{U}_1 \times_2 \mathbf{U}_2 \times_3 \mathbf{U}_3)] \times_2 \mathbf{U}_2^{\text{H}} \times_3 \mathbf{U}_3^{\text{H}}$$

Written in the first unfolding, the multiplication with \mathbf{U}_2^{H} and \mathbf{U}_3^{H} in, respectively, the second and third direction is equivalent to post-multiplication with the matrix $(\mathbf{I} \otimes \mathbf{U}_2^{\text{H}})^{\text{H}} (\mathbf{U}_3^{\text{H}} \otimes \mathbf{I})^{\text{H}} = (\mathbf{U}_3^{\text{H}} \otimes \mathbf{U}_2^{\text{H}})^{\text{H}} = (\mathbf{U}_3 \otimes \mathbf{U}_2)$.

Most of the terms are equal to the case where we had a constant wave number, see also (45). Let us focus on the last term that contains the Hadamard product with the space-dependent wave number, i.e.:

$$\mathcal{K} \circ (\mathcal{G} \times_1 \mathbf{U}_1 \times_2 \mathbf{U}_2 \times_3 \mathbf{U}_3). \quad (62)$$

For Hadamard products of tensors, $\mathcal{Z} = \mathcal{X} \circ \mathcal{Y}$, the following property for the k -th unfolding holds $\mathcal{Z}_{(k)} = \mathcal{X}_{(k)} \circ \mathcal{Y}_{(k)}$. Thus, written in the first unfolding (62) is given by

$$\begin{aligned} \mathbf{K}_{(1)} \circ \mathbf{M}_{(1)} \\ \mathbf{K}_{(1)} \circ \left(\overline{\mathbf{U}_1} \mathbf{G}_{(1)} (\mathbf{U}_3 \otimes \mathbf{U}_2)^{\text{H}} \right). \end{aligned} \quad (63)$$

As the Hadamard product-term (63) is written in the first unfolding and multiplication with \mathbf{U}_2^{H} and \mathbf{U}_3^{H} in respectively the second and third dimension results in

$$\left[\underbrace{\mathbf{K}_{(1)}}_{\mathbf{K}} \circ \underbrace{\overline{\mathbf{U}_1} \mathbf{G}_{(1)}}_{\mathbf{U}} \underbrace{(\mathbf{U}_3 \otimes \mathbf{U}_2)^{\text{H}}}_{\mathbf{V}^{\text{H}}} \right] \underbrace{(\mathbf{U}_3 \otimes \mathbf{U}_2)}_{\mathbf{V}}. \quad (64)$$

The derivation of the other terms of (61) are equal to the constant wave number case. The equation in the first unfolding leads to a matrix equation:

$$-\overline{\mathbf{D}_{xx}}\overline{\mathbf{U}_1}\mathbf{G}_{(1)}-\overline{\mathbf{U}_1}\mathbf{G}_{(1)}\left(\mathbf{I}\otimes\mathbf{U}_2^H\mathbf{D}_{yy}\mathbf{U}_2\right)^H-\overline{\mathbf{U}_1}\mathbf{G}_{(1)}\left(\mathbf{U}_3^H\mathbf{D}_{zz}\mathbf{U}_3\otimes\mathbf{I}\right)^H-\left[\mathbf{K}_{(1)}\circ\overline{\mathbf{U}_1}\mathbf{G}_{(1)}\left(\mathbf{U}_3\otimes\mathbf{U}_2\right)^H\right]\left(\mathbf{U}_3\otimes\mathbf{U}_2\right)=\mathbf{F}_{(1)}\left(\mathbf{U}_3\otimes\mathbf{U}_2\right) \quad (65)$$

Vectorization of the last term, i.e. (64), results again in an expression for the space-dependent wave number of the form $(\mathbf{K}\circ\mathbf{UV}^H)\mathbf{V}$, similar to the two dimensional case which was given in (25). Using again (27), the vectorization of this expression is given by

$$\left(\mathbf{U}_3^T\otimes\mathbf{U}_2^T\otimes\mathbf{I}\right)\text{diag}\left(\text{vec}\left[\mathbf{K}_{(1)}\right]\right)\overline{\left(\mathbf{U}_3\otimes\mathbf{U}_2\otimes\mathbf{I}\right)}\text{vec}\left[\overline{\mathbf{U}_1}\mathbf{G}_{(1)}\right]. \quad (66)$$

Because \mathbf{K} is known in a Canonical Polyadic tensor (CP tensor) decomposition², as given in (60), we have

$$\text{diag}\left(\text{vec}\left[\mathbf{K}_{(1)}\right]\right)=\sum_{i=1}^s\sigma_i\text{diag}\left(\mathbf{v}_i^{(3)}\right)\otimes\text{diag}\left(\mathbf{v}_i^{(2)}\right)\otimes\text{diag}\left(\mathbf{v}_i^{(1)}\right). \quad (67)$$

So, using the CP tensor representation of the space-dependent wave number the vectorization in (66) simplifies even further:

$$\sum_{i=1}^s\sigma_i\left(\mathbf{U}_3^T\otimes\mathbf{U}_2^T\otimes\mathbf{I}\right)\left[\text{diag}\left(\mathbf{v}_i^{(3)}\right)\otimes\text{diag}\left(\mathbf{v}_i^{(2)}\right)\otimes\text{diag}\left(\mathbf{v}_i^{(1)}\right)\right]\overline{\left(\mathbf{U}_3\otimes\mathbf{U}_2\otimes\mathbf{I}\right)}\text{vec}\left[\overline{\mathbf{U}_1}\mathbf{G}_{(1)}\right]$$

which reduced to

$$\underbrace{\sum_{i=1}^s\sigma_i\left(\mathbf{U}_3^T\text{diag}\left(\mathbf{v}_i^{(3)}\right)\overline{\mathbf{U}_3}\right)\otimes\left(\mathbf{U}_2^T\text{diag}\left(\mathbf{v}_i^{(2)}\right)\overline{\mathbf{U}_2}\right)\otimes\left(\text{diag}\left(\mathbf{v}_i^{(1)}\right)\right)}_{\mathbf{K}_1}\text{vec}\left[\overline{\mathbf{U}_1}\mathbf{G}_{(1)}\right].$$

In this way the \mathbf{K}_1 operator is defined and can be applied to $\text{vec}\left[\overline{\mathbf{U}_1}\mathbf{G}_{(1)}\right]$. Observe that this expansion is only advantageous if the space-dependent wave number has low rank, which is typical the case for our applications. In a similar way, the \mathbf{K}_2 and \mathbf{K}_3 operators can be derived:

$$\begin{aligned} \mathbf{K}_1 &= \sum_{i=1}^s\sigma_i\left(\mathbf{U}_3^T\text{diag}\left(\mathbf{v}_i^{(3)}\right)\overline{\mathbf{U}_3}\right)\otimes\left(\mathbf{U}_2^T\text{diag}\left(\mathbf{v}_i^{(2)}\right)\overline{\mathbf{U}_2}\right)\otimes\left(\text{diag}\left(\mathbf{v}_i^{(1)}\right)\right) \\ \mathbf{K}_2 &= \sum_{i=1}^s\sigma_i\left(\mathbf{U}_3^T\text{diag}\left(\mathbf{v}_i^{(3)}\right)\overline{\mathbf{U}_3}\right)\otimes\left(\mathbf{U}_1^T\text{diag}\left(\mathbf{v}_i^{(1)}\right)\overline{\mathbf{U}_1}\right)\otimes\left(\text{diag}\left(\mathbf{v}_i^{(2)}\right)\right) \\ \mathbf{K}_3 &= \sum_{i=1}^s\sigma_i\left(\mathbf{U}_2^T\text{diag}\left(\mathbf{v}_i^{(2)}\right)\overline{\mathbf{U}_2}\right)\otimes\left(\mathbf{U}_1^T\text{diag}\left(\mathbf{v}_i^{(1)}\right)\overline{\mathbf{U}_1}\right)\otimes\left(\text{diag}\left(\mathbf{v}_i^{(3)}\right)\right). \end{aligned} \quad (68)$$

So, we find the following linear system to solve for $\text{vec}\left[\overline{\mathbf{U}_1}\mathbf{G}_{(1)}\right]$:

$$\left\{-\mathbf{I}\otimes\overline{\mathbf{D}_{xx}}-\left[\overline{\left(\mathbf{I}\otimes\mathbf{U}_2^H\mathbf{D}_{yy}\mathbf{U}_2\right)}-\overline{\left(\mathbf{U}_3^H\mathbf{D}_{zz}\mathbf{U}_3\otimes\mathbf{I}\right)}\right]\otimes\mathbf{I}-\mathbf{K}_1\right\}\text{vec}\left[\underbrace{\overline{\mathbf{U}_1}\mathbf{G}_{(1)}}_{\mathbf{X}_1}\right]=\text{vec}\left[\mathbf{F}_{(1)}\left(\mathbf{U}_3\otimes\mathbf{U}_2\right)\right]. \quad (69)$$

Observe this is a square system with $n_1\times r_2r_3$ unknowns (where the solution in matrix form \mathbf{X}_1 is typical for rank $r>r_1$). In a similar way, update equations for \mathbf{U}_2 and \mathbf{U}_3 are derived by multiplying (61) with the other factor matrices in the appropriate directions:

$$\left\{-\mathbf{I}\otimes\overline{\mathbf{D}_{yy}}+\left[-\overline{\left(\mathbf{I}\otimes\mathbf{U}_1^H\mathbf{D}_{xx}\mathbf{U}_1\right)}-\overline{\left(\mathbf{U}_3^H\mathbf{D}_{zz}\mathbf{U}_3\otimes\mathbf{I}\right)}\right]\otimes\mathbf{I}-\mathbf{K}_2\right\}\text{vec}\left[\underbrace{\overline{\mathbf{U}_2}\mathbf{G}_{(2)}}_{\mathbf{X}_2}\right]=\text{vec}\left[\mathbf{F}_{(2)}\left(\mathbf{U}_3\otimes\mathbf{U}_1\right)\right]. \quad (70)$$

²Otherwise a Canonical Polyadic tensor decomposition can be computed using for example an CP-ALS algorithm [12].

Algorithm 5: Solve for the low-rank tensor decomposition of the solution \mathcal{M} of a 3D Helmholtz problem with space-dependent wave number (version 1).

```

1  $[\mathcal{G}, \mathbf{U}_1, \mathbf{U}_2, \mathbf{U}_3] = \text{hosvd}(\text{initial guess});$ 
2  $[\Sigma, \mathbf{V}_1, \mathbf{V}_2, \mathbf{V}_3] = \text{cp\_als}(\mathcal{K});$ 
3 while not converged do
4   for  $i = 1, 2, 3$  do
5     Compute  $K_i$  using (68);
6     Solve for  $\mathbf{X}_i = \overline{\mathbf{U}}_i \mathbf{G}_{(i)} \in \mathbb{C}^{n_i \times r^{d-1}}$  using (69), (70) or (71);
7      $\overline{\mathbf{U}}_i \mathbf{G}_{(i)} = \text{qr}[\mathbf{X}_i(:, 1:r_i), 0];$ 
8   end
9 end
10  $\mathcal{G} = \text{reconstruct}[\mathbf{G}_{(i)}, i];$ 
11  $\mathcal{M} = \mathcal{G} \times_1 \mathbf{U}_1 \times_2 \mathbf{U}_2 \times_3 \mathbf{U}_3;$ 

```

and

$$\left\{ -I \otimes \overline{D_{zz}} + \left[-\overline{(I \otimes \mathbf{U}_1^H D_{xx} \mathbf{U}_1)} - \overline{(\mathbf{U}_2^H D_{yy} \mathbf{U}_2 \otimes I)} \right] \otimes I - K_3 \right\} \text{vec} \left[\underbrace{\overline{\mathbf{U}}_3 \mathbf{G}_{(3)}}_{\mathbf{X}_3} \right] = \text{vec} [\mathbf{F}_{(3)} (\mathbf{U}_2 \otimes \mathbf{U}_1)]. \quad (71)$$

Alternating between solving for \mathbf{U}_1 , \mathbf{U}_2 and \mathbf{U}_3 using (69), (70) or (71) results in an algorithm to approximate low-rank tensor solutions for three dimensional problems as given in (41). Also in this case the orthogonality of the columns of \mathbf{U}_1 , \mathbf{U}_2 and \mathbf{U}_3 are maintained by additional QR factorizations. So, we derive the algorithm as formulated in Algorithm 5. The generalization for dimensions $d > 3$ is straight forward.

Similar to the discussion for the constant wave number algorithms, observe that we solve again for a large matrix $\mathbf{X}_i \in \mathbb{C}^{n_i \times r_1 r_2 r_3 / r_i}$. So, in general the rank of this matrix could be $\min(n_i, r_1 r_2 r_3 / r_i)$. But it is also known that $\mathbf{X}_i = \overline{\mathbf{U}}_i \mathbf{G}_{(i)}$ leads to the fact that the rank of \mathbf{X}_i should be at most r_i . So selecting the first r_i columns of \mathbf{X}_i and computing its QR decomposition is sufficient to derive a new orthonormal basis as factor matrix $\overline{\mathbf{U}}_i$.

Algorithm 5 is exactly the space-dependent wave number equivalent of Algorithm 2. The same ideas can be applied to derive space-dependent wave number alternatives of the algorithms corresponding to version 2 and 3. Again, to circumvent solving large systems, we can pre-compute the QR factorization of $\mathbf{G}_{(i)}$ and project these equations onto the obtained \mathbf{Q}_i . Indeed, this will reduce the number of unknowns in these linear systems to exactly the number of unknowns as needed for the factor matrices $\overline{\mathbf{U}}_1$ and $\overline{\mathbf{U}}_2$.

Let us discuss the details. We start again from equation (65) and use the QR factorization of $\mathbf{G}_{(1)}^H$, $\mathbf{Q}_1 \mathbf{R}_1^H = \text{qr}[\mathbf{G}_{(1)}^H]$. This yields

$$-\overline{D_{xx} \mathbf{U}_1 \mathbf{R}_1 \mathbf{Q}_1^H} - \overline{\mathbf{U}_1 \mathbf{R}_1 \mathbf{Q}_1^H} (I \otimes \mathbf{U}_2^H D_{yy} \mathbf{U}_2)^H - \overline{\mathbf{U}_1 \mathbf{R}_1 \mathbf{Q}_1^H} (\mathbf{U}_3^H D_{zz} \mathbf{U}_3 \otimes I)^H - \left[\mathbf{K}_{(1)} \circ \overline{\mathbf{U}_1 \mathbf{R}_1 \mathbf{Q}_1^H} (\mathbf{U}_3 \otimes \mathbf{U}_2)^H \right] (\mathbf{U}_3 \otimes \mathbf{U}_2) = \mathbf{F}_{(1)}$$

Post multiplication of the left hand side of this equation by \mathbf{Q}_1 yields

$$-\overline{D_{xx} \mathbf{U}_1 \mathbf{R}_1} - \overline{\mathbf{U}_1 \mathbf{R}_1 \mathbf{Q}_1^H} (I \otimes \mathbf{U}_2^H D_{yy} \mathbf{U}_2)^H \mathbf{Q}_1 - \overline{\mathbf{U}_1 \mathbf{R}_1 \mathbf{Q}_1^H} (\mathbf{U}_3^H D_{zz} \mathbf{U}_3 \otimes I)^H \mathbf{Q}_1 - \left[\mathbf{K}_{(1)} \circ \overline{\mathbf{U}_1 \mathbf{R}_1 \mathbf{Q}_1^H} (\mathbf{U}_3 \otimes \mathbf{U}_2)^H \right] (\mathbf{U}_3 \otimes \mathbf{U}_2) \mathbf{Q}_1.$$

To solve this equation for \mathbf{U}_1 , it is written in vectorized form as

$$\left\{ -I \otimes \overline{D_{xx}} + \mathbf{Q}_1^T \left[-\overline{(I \otimes \mathbf{U}_2^H D_{yy} \mathbf{U}_2)} - \overline{(\mathbf{U}_3^H D_{zz} \mathbf{U}_3 \otimes I)} \right] \mathbf{Q}_1 \otimes I - \mathbf{Q}_1^T \mathbf{K}_1 \mathbf{Q}_1 \right\} \text{vec} \left[\underbrace{\overline{\mathbf{U}}_1 \mathbf{R}_1}_{\mathbf{X}_1} \right] = \text{vec} [\mathbf{F}_{(1)} (\mathbf{U}_3 \otimes \mathbf{U}_2) \mathbf{Q}_1]. \quad (72)$$

In a similar way, the update equations for \mathbf{U}_2 and \mathbf{U}_3 are derived by multiplying (61) with the other factor matrices in the appropriate dimensions and using the QR factorizations of $\mathbf{G}_{(i)}^H$:

$$\left\{ -I \otimes \overline{D_{yy}} + \mathbf{Q}_2^T \left[-\overline{(I \otimes \mathbf{U}_1^H D_{xx} \mathbf{U}_1)} - \overline{(\mathbf{U}_3^H D_{zz} \mathbf{U}_3 \otimes I)} \right] \mathbf{Q}_2 \otimes I - \mathbf{Q}_2^T \mathbf{K}_2 \mathbf{Q}_2 \right\} \text{vec} \left[\underbrace{\overline{\mathbf{U}}_2 \mathbf{R}_2}_{\mathbf{X}_2} \right] = \text{vec} [\mathbf{F}_{(2)} (\mathbf{U}_3 \otimes \mathbf{U}_1) \mathbf{Q}_2]. \quad (73)$$

Algorithm 6: Solve for the low-rank tensor decomposition of the solution \mathcal{M} of a 3D Helmholtz problem with space-dependent wave number (version 3).

```

1  $[\mathcal{G}, \mathbf{U}_1, \mathbf{U}_2, \mathbf{U}_3] = \text{hosvd}(\text{initial guess});$ 
2  $[\Sigma, \mathbf{V}_1, \mathbf{V}_2, \mathbf{V}_3] = \text{cp\_als}(\mathcal{K});$ 
3 while not converged do
4   for  $i = 1, 2$  do
5     Compute  $K_i$  using (68);
6      $\mathbf{Q}_i \tilde{\mathbf{R}} = \text{qr} [\mathbf{G}_{(i)}^H, 0];$ 
7     Solve for  $\mathbf{X}_i = \overline{\mathbf{U}}_i \mathbf{R}_i \in \mathbb{C}^{n_i \times r_i}$  using (72) or (73);
8      $\overline{\mathbf{U}}_i \mathbf{R}_i = \text{qr} [\mathbf{X}_i, 0];$ 
9      $\mathcal{G} = \text{reconstruct} [\mathbf{R}_i \mathbf{Q}_i^H, i];$ 
10  end
11  Compute  $K_3$  using (68);
12  Solve for  $\mathbf{X}_3 = \overline{\mathbf{U}}_3 \mathbf{G}_{(3)} \in \mathbb{C}^{n_3 \times r^{d-1}}$  using (71);
13   $\overline{\mathbf{U}}_3 \mathbf{G}_{(3)} = \text{qr} [\mathbf{X}_3, 0];$ 
14   $\mathcal{G} = \text{reconstruct} [\mathbf{G}_{(3)}, 3];$ 
15 end
16  $\mathcal{M} = \mathcal{G} \times_1 \mathbf{U}_1 \times_2 \mathbf{U}_2 \times_3 \mathbf{U}_3;$ 

```

and

$$\left\{ -\mathbf{I} \otimes \overline{\mathbf{D}}_{zz} + \mathbf{Q}_3^T \left[-(\overline{\mathbf{I} \otimes \mathbf{U}_1^H \mathbf{D}_{xx} \mathbf{U}_1}) - (\overline{\mathbf{U}_2^H \mathbf{D}_{yy} \mathbf{U}_2 \otimes \mathbf{I}}) \right] \overline{\mathbf{Q}}_3 \otimes \mathbf{I} \right\} \text{vec} \left[\underbrace{\overline{\mathbf{U}_3 \mathbf{R}_3}}_{\mathbf{X}_3} \right] - \mathbf{Q}_3^T K_3 \overline{\mathbf{Q}}_3 = \text{vec} [\mathbf{F}_{(3)} (\mathbf{U}_2 \otimes \mathbf{U}_1) \mathbf{Q}_3]. \quad (74)$$

All these equations are cheap to solve. Indeed, $\text{vec} [\overline{\mathbf{U}}_i \mathbf{R}_i]$ has length $n_i r_i$. Computing a symmetric reverse Cuthill-McKee permutation of the system matrix one observes a matrix with a bandwidth $\mathcal{O}(r)$, so solving these equations has a computational cost $\mathcal{O}(nr^2)$.

Alternating between solving for \mathbf{U}_1 , \mathbf{U}_2 and \mathbf{U}_3 using (72), (73) or (71) results again in an algorithm to approximate low-rank solutions for three dimensional space-dependent Helmholtz problems. Also in this case the orthogonality of the columns of \mathbf{U}_1 , \mathbf{U}_2 and \mathbf{U}_3 are maintained by additional QR factorizations. So, we derive the algorithm as formulated in Algorithm 6. Algorithm 6 is exactly the space-dependent wave number equivalent of Algorithm 4.

4.4 Projection operator for space-dependent wave number

Consider a tensor \mathcal{M} in Tucker tensor format and factorized as $\mathcal{M} = \mathcal{G} \times_1 \mathbf{U}_1 \times_2 \mathbf{U}_2 \times_3 \mathbf{U}_3$, with unknowns $\mathcal{G}, \mathbf{U}_1, \mathbf{U}_2$ and \mathbf{U}_3 . Discretization of (41) with a space-dependent wave number leads to a linear operator \mathcal{L} applied on tensors. Its matrix representation \mathbf{L} has again a structure as given in (44).

Solving for the unknown factors \mathbf{U}_1 , \mathbf{U}_2 or \mathbf{U}_3 (and the core-tensor \mathcal{G}) using (69), (70) or (71) can, again, be interpreted as a projection operator applied on the residual. For example, (69) can be interpreted as

$$\overline{(\mathbf{U}_3^H \otimes \mathbf{U}_2^H \otimes \mathbf{I}) \mathbf{L} (\mathbf{U}_3 \otimes \mathbf{U}_2 \otimes \mathbf{I})} \text{vec} [\overline{\mathbf{U}}_1 \mathbf{G}_{(1)}] = (\mathbf{U}_3^T \otimes \mathbf{U}_2^T \otimes \mathbf{I}) \text{vec} [\mathbf{F}_{(1)}], \quad (75)$$

The residual in tensor format is given by

$$\begin{aligned} \mathcal{R} &= \mathcal{F} - \mathcal{L}\mathcal{M}, \\ &= \mathcal{F} + \mathcal{G} \times_1 \mathbf{D}_{xx} \mathbf{U}_1 \times_2 \mathbf{U}_2 \times_3 \mathbf{U}_3 \\ &\quad + \mathcal{G} \times_1 \mathbf{U}_1 \times_2 \mathbf{D}_{yy} \mathbf{U}_2 \times_3 \mathbf{U}_3 \\ &\quad + \mathcal{G} \times_1 \mathbf{U}_1 \times_2 \mathbf{U}_2 \times_3 \mathbf{D}_{zz} \mathbf{U}_3 \\ &\quad + \mathcal{K} \circ (\mathcal{G} \times_1 \mathbf{U}_1 \times_2 \mathbf{U}_2 \times_3 \mathbf{U}_3). \end{aligned} \quad (76)$$

Writing this tensor equation in the first unfolding leads to the following matrix equation

$$\begin{aligned}
\mathbf{R}_{(1)} &= \mathbf{F}_{(1)} + \overline{\mathbf{D}_{xx}\mathbf{U}_1\mathbf{G}_{(1)}} (\mathbf{U}_3 \otimes \mathbf{U}_2)^{\text{H}} \\
&\quad + \overline{\mathbf{U}_1\mathbf{G}_{(1)}} (\mathbf{U}_3 \otimes \mathbf{D}_{yy}\mathbf{U}_2)^{\text{H}} \\
&\quad + \overline{\mathbf{U}_1\mathbf{G}_{(1)}} (\mathbf{D}_{zz}\mathbf{U}_3 \otimes \mathbf{U}_2)^{\text{H}} \\
&\quad + \mathbf{K}_{(1)} \circ \left(\overline{\mathbf{U}_1\mathbf{G}_{(1)}} (\mathbf{U}_3 \otimes \mathbf{U}_2)^{\text{H}} \right)
\end{aligned} \tag{77}$$

which can be matricized as

$$\begin{aligned}
\text{vec} [\mathbf{R}_{(1)}] &= \text{vec} [\mathbf{F}_{(1)}] \\
&\quad - \left(-\overline{(\mathbf{U}_3 \otimes \mathbf{U}_2 \otimes \mathbf{D}_{xx})} - \overline{(\mathbf{U}_3 \otimes \mathbf{D}_{yy}\mathbf{U}_2 \otimes \mathbf{I})} - \overline{(\mathbf{D}_{zz}\mathbf{U}_3 \otimes \mathbf{U}_2 \otimes \mathbf{I})} - \text{diag}(\text{vec} [\mathbf{K}_{(1)}]) \overline{(\mathbf{U}_3 \otimes \mathbf{U}_2 \otimes \mathbf{I})} \right) \text{vec} [\overline{\mathbf{U}_1\mathbf{G}_{(1)}}]
\end{aligned}$$

Rewriting this results in exactly the same structure and projection operator as in the constant wave number case:

$$\begin{aligned}
\text{vec} [\mathbf{R}_{(1)}] &= \dots \\
&= \text{vec} [\mathbf{F}_{(1)}] - \overline{\mathbf{L}(\mathbf{U}_3 \otimes \mathbf{U}_2 \otimes \mathbf{I})} \text{vec} [\overline{\mathbf{U}_1\mathbf{G}_{(1)}}] \\
&= \text{vec} [\mathbf{F}_{(1)}] - \overline{\mathbf{L}(\mathbf{U}_3 \otimes \mathbf{U}_2 \otimes \mathbf{I})} \left[\overline{(\mathbf{U}_3^{\text{H}} \otimes \mathbf{U}_2^{\text{H}} \otimes \mathbf{I}) \mathbf{L}(\mathbf{U}_3 \otimes \mathbf{U}_2 \otimes \mathbf{I})} \right]^{-1} (\mathbf{U}_3^{\text{T}} \otimes \mathbf{U}_2^{\text{T}} \otimes \mathbf{I}) \text{vec} [\mathbf{F}_{(1)}] \\
&= P_{23} \text{vec} [\mathbf{F}_{(1)}]
\end{aligned} \tag{78}$$

where projection operator P_{23} is similar to the projector in the constant wave number case, see (58), and now given by

$$\begin{aligned}
P_{23} &= \mathbf{I} - \overline{\mathbf{L}(\mathbf{U}_3 \otimes \mathbf{U}_2 \otimes \mathbf{I})} \left[\overline{(\mathbf{U}_3^{\text{H}} \otimes \mathbf{U}_2^{\text{H}} \otimes \mathbf{I}) \mathbf{L}(\mathbf{U}_3 \otimes \mathbf{U}_2 \otimes \mathbf{I})} \right]^{-1} (\mathbf{U}_3^{\text{T}} \otimes \mathbf{U}_2^{\text{T}} \otimes \mathbf{I}) \\
&= \mathbf{I} - \mathbf{X}.
\end{aligned} \tag{79}$$

A similar derivation results in projection operators P_{13} and P_{12} for the updates in \mathbf{U}_2 and \mathbf{U}_3 , respectively. Both are also the same as in the constant wave number case, as given in (59).

5 Numerical results

In this section, we demonstrate the promising results of the derived algorithms with some numerical experiments in two and three dimensions. Furthermore, we consider discretizations of the Helmholtz equation with constant and space-dependent wave numbers.

5.1 2D Helmholtz problem with space-dependent wave number

First, we consider a 2D Helmholtz problem with a space-dependent wave number given by $k^2(x, y) = 2 + e^{-x^2 - y^2}$. For this example the two dimensional domain $\Omega = [-10, 10]^2$ is discretized with $M = 1000$ equidistant mesh points per direction in the interior of the domain. Further it is extended with exterior complex scaling to implement the absorbing boundary conditions. In total, the number of discretization points per directions equals $n = n_1 = n_2 = 1668$. As external force $f(x, y) = -e^{-x^2 - y^2}$ is applied.

In this space-dependent wave number example it is known that the matrix representation of the semi-exact solution of the Helmholtz equation on the full grid has a low rank. Indeed, approximating the semi-exact solution with a low-rank matrix with rank $r = 17$ is in this case sufficient to obtain an error below the threshold $\tau = 10^{-6}$.

Starting with an random (orthonormalized) initial guess for $\mathbf{V}^{(0)} \in \mathbb{C}^{n \times r}$ only a small number of iterations of Algorithm 1 is needed to obtain an error similar to the specified threshold τ . As shown in Figure 8 both the residual and the error with respect to the semi-exact solution decay in only a few iterations (i.e. in this example 4-8 iterations) to a level almost similar to the expected tolerance.

The singular values of the approximation $\mathbf{A}^{(k)} = \mathbf{U}^{(k)} \mathbf{R}^{(k)\text{H}} \mathbf{V}^{(k)\text{H}}$ in iteration i can be computed and are shown for increasing iterations in Figure 8. As expected the low-rank approximations recover the singular values of the full grid semi-exact solution. In fact $\mathbf{R}^{(k)}$ converges towards $\text{diag}(\sigma_i)$.

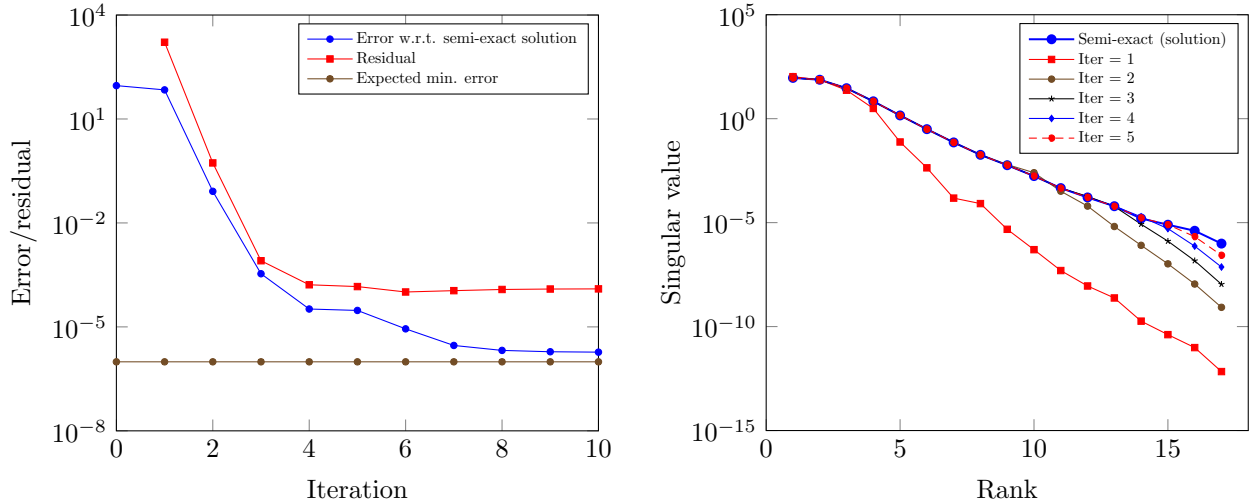


Figure 8: Plot of error and residual (left) and singular values (right) per iteration for space-dependent wave number in 2D Helmholtz problem ($M = 1000, r = 17$).

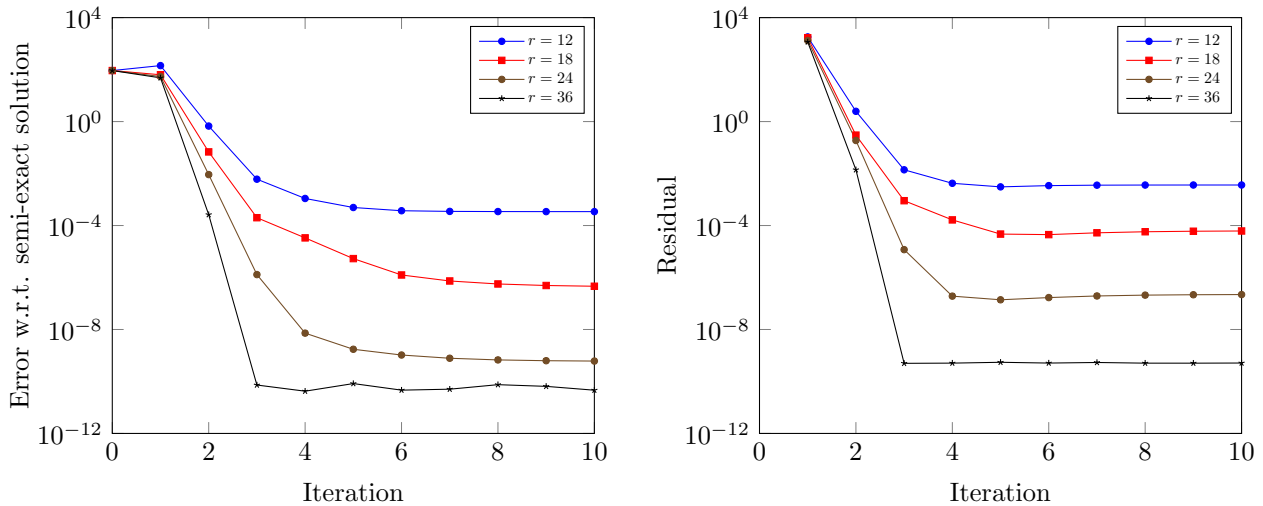


Figure 9: Plot of errors (left) and residuals (right) per iteration for space-dependent wave number in 2D Helmholtz problem with increasing ranks ($M = 1000$)

The numerical rank of the matrix representation of the solution of a Helmholtz problem with a space-dependent wave number is unknown in advance. But, the presented algorithm is stable with respect to over- and underestimation of the numerical rank of the solution. Figure 9 shows both the error and residual per iteration and illustrates this statement by approximating the same semi-exact solution with increasing ranks $r \in \{12, 18, 24, 36\}$. In contrast to the constant coefficient wave number case the convergence with space-dependent wave number depends also on the maximal attainable rank. For increasing maximal attainable ranks the number of needed iterations decreases. This is especially observed when the error is considered, but it can also be seen in the figure where the residuals are shown, Fig. 9.

5.2 3D Helmholtz problem with space-dependent wave number

In this example we solve a 3D Helmholtz problem with a space-dependent wave number discretized on a DVR-grid [20]. All three versions of the 3D algorithm for space-dependent wave numbers can successfully be applied. First, to reduce computational cost of construction of the operators K_1 , K_2 and K_3 , see (68), a CP-decomposition of the space-dependent wave number is constructed. As shown in Figure 11a the space-dependent wave number can be well-approximated by a small number of rank-1 tensors. For the examples discussed in this section we used a CP-rank $s = 32$ to approximate this space-dependent wave number. Hence, the error in approximating

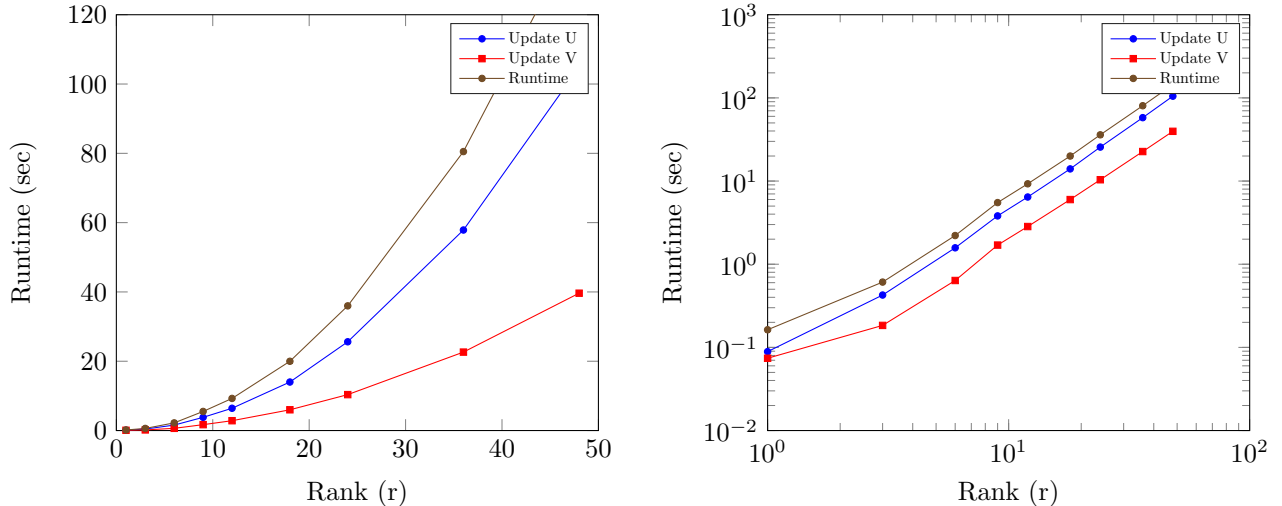


Figure 10: Plot of runtime for 10 iterations for space-dependent wave number in 2D Helmholtz problem with increasing ranks ($M = 1000$). Left: linlin-scale, right: loglog-scale.

the wave number is approximately $\mathcal{O}(10^{-4})$.

For all three versions of the algorithm we use 10 iterations of the algorithm to converge to the low-rank solution. For example if we compute the low-rank solution (with $r = r_x = r_y = r_z = 16$) the residual after each iteration for all algorithms is shown in Figure 11b.

If we increase the maximal attainable rank r of the low-rank approximation, indeed the residual decreases as shown in Figure 12a. The residual for version 1 and version 3 are good, while version 2 cannot compete with both other versions by reducing the residual as far as the other versions. Therefore version 1 or version 3, as given in Algorithm 5 or Algorithm 6 are preferred.

Considering the runtimes of the three versions, similar results as before are observed. In this experiment with $\text{orderDvr}=7$ the number of gridpoints equals to $n = 41$. For version 1 and 3, again a runtime of $\mathcal{O}(nr^4)$ is observed. The runtime for version 2 splits into two parts: $\mathcal{O}(nr^2 + r^9)$. Due to the small rank r and the large number of iterations in these examples algorithm 2 is the fastest version. The runtimes for version 1 and version 3 differ indeed approximately a factor d , which makes version 3 better than version 1. The runtimes with $\text{orderDvr} = 7$ (i.e. $n = 41$) are shown in Figure 13a and with $\text{orderDvr} = 14$ (i.e. $n = 90$) are shown in Figure 13b.

Comparing the runtimes for $\text{orderDvr}=7$ and $\text{orderDvr}=14$ we see for version 2 (when the rank gets larger) indeed approximately the same runtime independent of orderDvr . Also versions 1 and 3 consume approximately twice as much time which is as expected by the linear dependence on n for both algorithms.

An impression of the low-rank approximation to the wave function is shown in Figures 14b and 15. In this impression the single, double and triple ionization are visible and can be represented by a low-rank wave function.

6 Discussion and conclusions

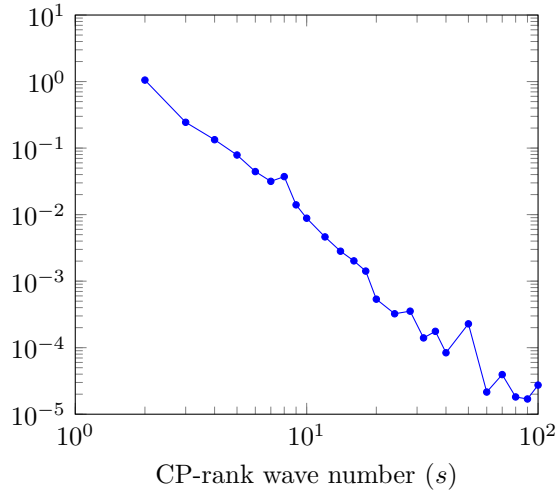
In this paper we have analyzed the scattering solutions of a driven Schrödinger equations. These describe a break-up reaction where a quantum system is fragmented into multiple fragments. These problems are equivalent to solving a Helmholtz equations with space-dependent wave numbers.

We have shown, first in 2D and then in 3D, that the wave function of multiple ionization can be well approximated by a low-rank solution. In 2D, the waves can be represented as a product of two low-rank matrices and 3D as a low-rank Tucker tensor decomposition.

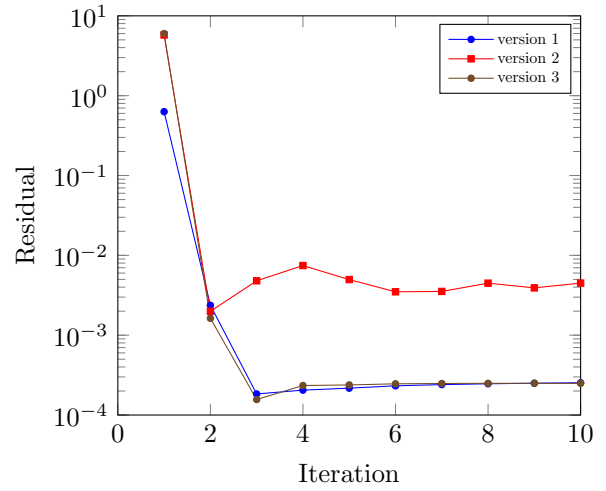
We propose a method that determines these low-rank components of the solution directly. We write the solution as a product of low-rank components and assume that a guess for all but one component is given. We then write a linear system for the remaining unknown component. This is repeated until each of the components is updated.

This procedure can be interpreted as a series of projections of the residual on a subspaces and a correction within that subspace.

In theory, the generalization for dimensions $d > 3$ is straightforward. But for dimensions $d > 3$ it starts to be beneficial to change to a Tensor Train factorization [17]. It is expected that similar strategy can also be applied

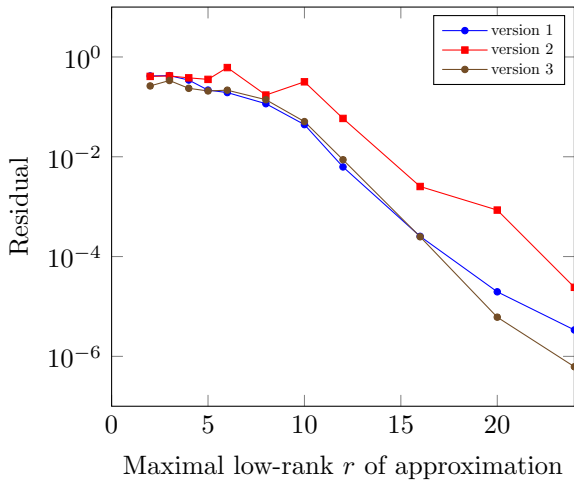


(a) CP-rank of space-dependent wave number for 3D Helmholtz problem.

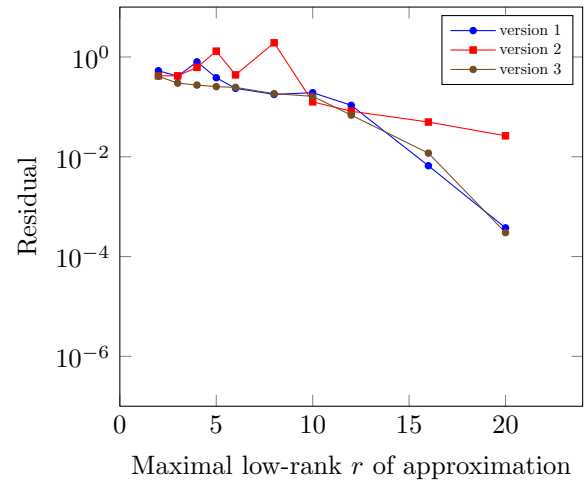


(b) Residual per iteration ($r = 16, s = 32$).

Figure 11: Low rank approximation to space-dependent wave number and residuals for version 1, version 2 and version 3 of 3D Helmholtz problem with space-dependent wave number ($\text{orderDvr} = 7$).



(a) $\text{orderDvr} = 7$



(b) $\text{orderDvr} = 14$

Figure 12: Residual after iteration 10 iterations for all three versions of algorithm with $s = 32$.

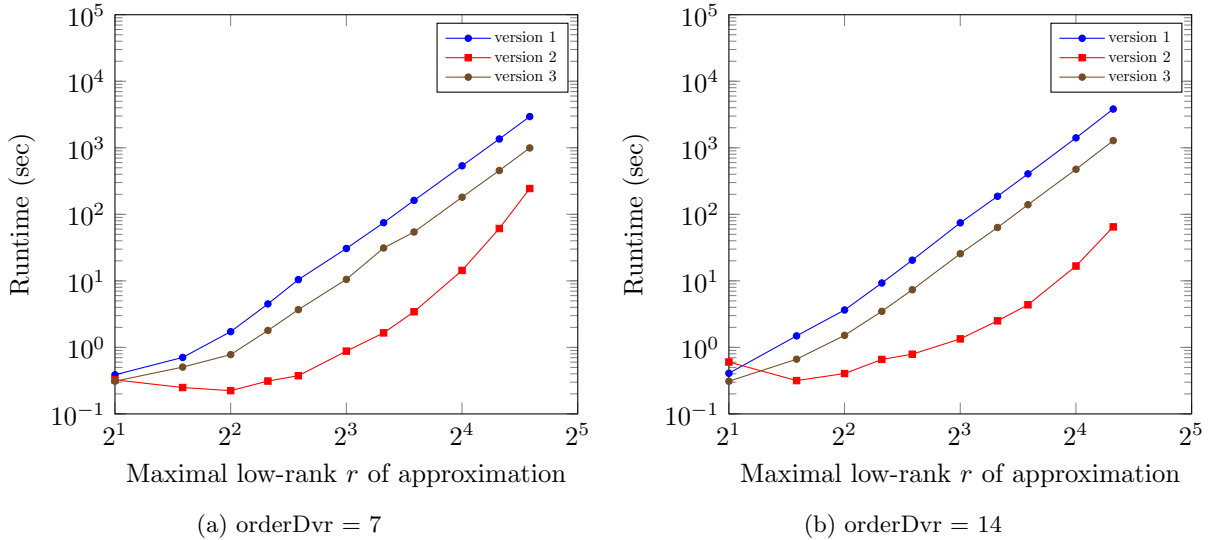


Figure 13: Runtime of 10 iterations for all three versions of algorithm for 3D Helmholtz with space-dependent wave number of low-rank $s = 32$.

to tensors in Tensor Train format.

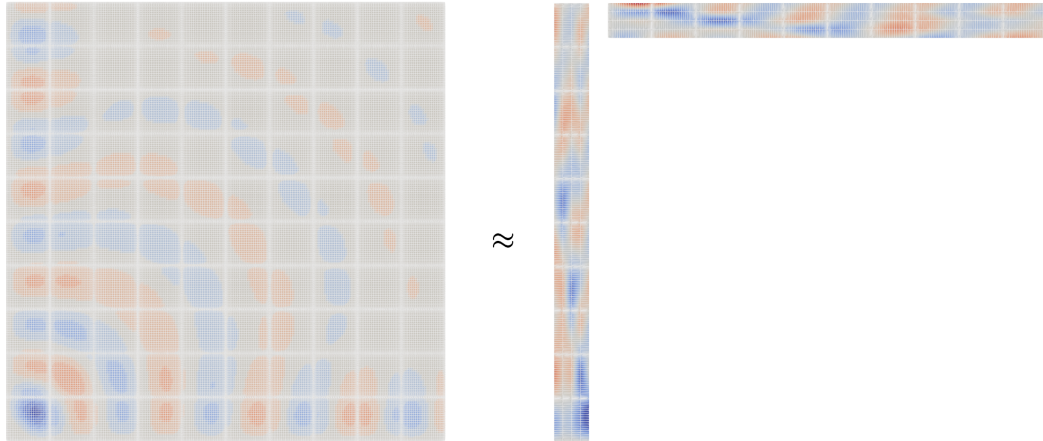
As demonstrated by the numerical experiments, the presented algorithms are able to exploit the low-rank structure of the solutions. This gives the advantage to reduce the number of unknowns and shorten the computational time to solve the Helmholtz equation.

In two dimensions, the low-rank representation of the solution can be represented by only $2nr$ unknowns instead of the full grid of n^2 unknowns. Also the linear systems to solve per iteration have only nr unknowns.

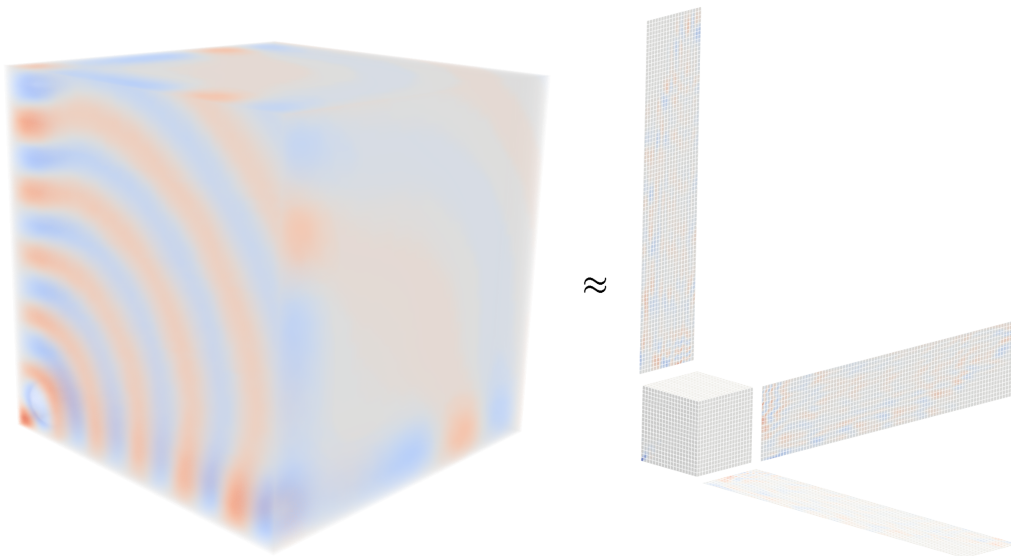
In high-dimensional Helmholtz equations, the low-rank Tucker tensor decomposition represents the solution with $\mathcal{O}(r^d + dnr)$ unknowns. So, the total number of unknowns is reduced, but it is still exponential in the dimension d . For increasing dimensions this leads, again, to systems with a number of unknowns exponential in d . Maybe other Tucker-like tensor decompositions with a number of unknowns only polynomial in d can resolve this problem and make the presented algorithm also applicable for higher dimensions.

References

- [1] Dominique Akoury, K Kreidi, T Jahnke, Th Weber, A Staudte, M Schoffler, N Neumann, J Titze, L Ph H Schmidt, A Czasch, et al. The simplest double slit: interference and entanglement in double photoionization of H₂. *Science*, 318(5852):949–952, 2007.
- [2] Jean-Pierre Berenger. A perfectly matched layer for the absorption of electromagnetic waves. *Journal of computational physics*, 114(2):185–200, 1994.
- [3] JS Briggs and V Schmidt. Differential cross sections for photo-double-ionization of the helium atom. *Journal of Physics B: Atomic, Molecular and Optical Physics*, 33(1):R1, 2000.
- [4] Weng Cho Chew and William H Weedon. A 3D perfectly matched medium from modified Maxwell’s equations with stretched coordinates. *Microwave and optical technology letters*, 7(13):599–604, 1994.
- [5] Siegfried Cools and Wim Vanroose. A fast and robust computational method for the ionization cross sections of the driven Schrödinger equation using an $\mathcal{O}(n)$ multigrid-based scheme. *Journal of Computational Physics*, 308:20–39, 2016.
- [6] Sergey V Dolgov and Dmitry V Savostyanov. Alternating minimal energy methods for linear systems in higher dimensions. *SIAM Journal on Scientific Computing*, 36(5):A2248–A2271, 2014.
- [7] André Gaul and Nico Schlömer. Preconditioned recycling Krylov subspace methods for self-adjoint problems. *arXiv preprint arXiv:1208.0264*, 2012.
- [8] Lars Grasedyck, Daniel Kressner, and Christine Tobler. A literature survey of low-rank tensor approximation techniques. *GAMM-Mitteilungen*, 36(1):53–78, 2013.



(a) Impression of a low-rank matrix approximation in 2D.



(b) Impression of a low-rank tensor approximation in 3D.

Figure 14: Impressions of a low-rank approximation of a matrix and a Tucker tensor representing the wave function as solution to a 2D and 3D Helmholtz problem with a space-dependent wave number.

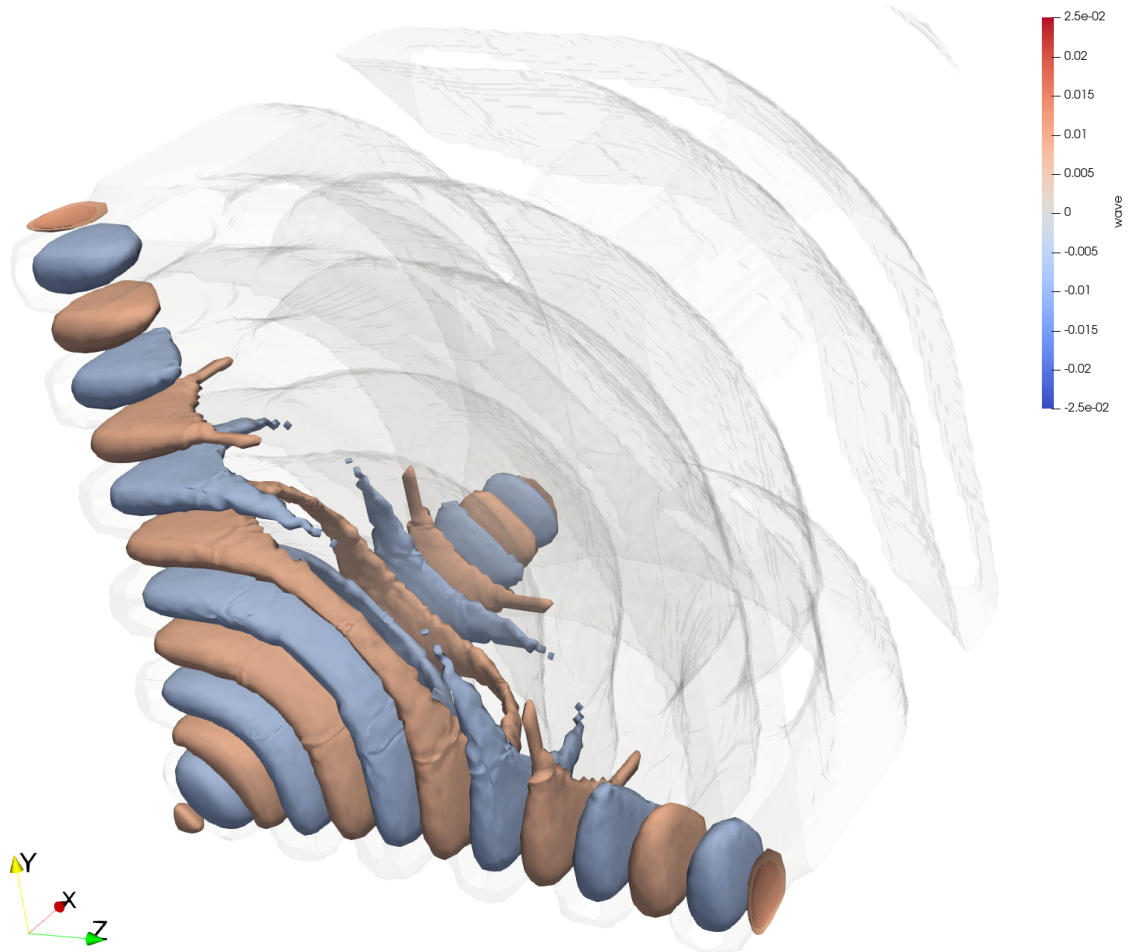


Figure 15: Visualization of a 3D wave as low-rank approximation to a 3D Helmholtz problem with space-dependent wave number with single, double and triple ionization.

- [9] Wolfgang Hackbusch. *Tensor spaces and numerical tensor calculus*, volume 42. Springer, 2012.
- [10] Sebastian Holtz, Thorsten Rohwedder, and Reinhold Schneider. The alternating linear scheme for tensor optimization in the tensor train format. *SIAM Journal on Scientific Computing*, 34(2):A683–A713, 2012.
- [11] Thomas Huckle, Konrad Waldherr, and Thomas Schulte-Herbrüggen. Computations in quantum tensor networks. *Linear Algebra and its Applications*, 438(2):750–781, 2013.
- [12] Tamara G Kolda and Brett W Bader. Tensor decompositions and applications. *SIAM review*, 51(3):455–500, 2009.
- [13] C William McCurdy, M Baertschy, and TN Rescigno. Solving the three-body coulomb breakup problem using exterior complex scaling. *Journal of Physics B: Atomic, Molecular and Optical Physics*, 37(17):R137, 2004.
- [14] Valentin Murg, Frank Verstraete, Örs Legeza, and Reinhard M Noack. Simulating strongly correlated quantum systems with tree tensor networks. *Physical Review B*, 82(20):205105, 2010.
- [15] J Neumann. Functional operators vol. ii. the geometry of orthogonal spaces. *annals of mathematical studies# 22*. 1950.
- [16] Ivan Oseledets. DMRG approach to fast linear algebra in the TT-format. *Computational Methods in Applied Mathematics*, 11(3):382–393, 2011.
- [17] Ivan V Oseledets. Tensor-train decomposition. *SIAM Journal on Scientific Computing*, 33(5):2295–2317, 2011.
- [18] R Poet. The exact solution for a simplified model of electron scattering by hydrogen atoms. *Journal of Physics B: Atomic and Molecular Physics*, 11(17):3081, 1978.
- [19] TN Rescigno, M Baertschy, WA Isaacs, and CW McCurdy. Collisional breakup in a quantum system of three charged particles. *Science*, 286(5449):2474–2479, 1999.
- [20] TN Rescigno and CW McCurdy. Numerical grid methods for quantum-mechanical scattering problems. *Physical review A*, 62(3):032706, 2000.
- [21] H Schmidt-Böcking, R Dörner, and J Ullrich. Coltrims. *Europhysics News*, 33(6):210–211, 2002.
- [22] Barry Simon. The definition of molecular resonance curves by the method of exterior complex scaling. *Physics Letters A*, 71(2-3):211–214, 1979.
- [23] Zachary L Streeter, Frank L Yip, Robert R Lucchese, Benoit Gervais, Thomas N Rescigno, and C William McCurdy. Dissociation dynamics of the water dication following one-photon double ionization. i. Theory. *Physical Review A*, 98(5):053429, 2018.
- [24] Aaron Temkin. Nonadiabatic theory of electron-hydrogen scattering. *Physical Review*, 126(1):130, 1962.
- [25] Ledyard R Tucker. Some mathematical notes on three-mode factor analysis. *Psychometrika*, 31(3):279–311, 1966.
- [26] Wim Vanroose, Daniel A Horner, Fernando Martin, Thomas N Rescigno, and C William McCurdy. Double photoionization of aligned molecular hydrogen. *Physical Review A*, 74(5):052702, 2006.
- [27] Wim Vanroose, Fernando Martin, Thomas N Rescigno, and C William McCurdy. Complete photo-induced breakup of the H₂ molecule as a probe of molecular electron correlation. *Science*, 310(5755):1787–1789, 2005.
- [28] Jinchao Xu and Ludmil Zikatanov. The method of alternating projections and the method of subspace corrections in Hilbert space. *Journal of the American Mathematical Society*, 15(3):573–597, 2002.